ELSEVIER

Cancer Genetics and Cytogenetics 180 (2008) 74–78

CANCER GENETICS AND CYTOGENETICS

Short communication

Mutations of *GATA1*, *FLT3*, *MLL*-partial tandem duplication, *NRAS*, and *RUNX1* genes are not found in a 7-year-old Down syndrome patient with acute myeloid leukemia (FAB-M2) having a good prognosis

Machiko Kawamura[a,*], Hidefumi Kaku[a], Takeshi Taketani[b], Tomohiko Taki[c], Akira Shimada[d], Yasuhide Hayashi[d]

[a]*Department of Pediatrics, Tokyo Metropolitan Komagome Hospital, 3-18-22 Honkomagome, Bunkyo-ku, Tokyo 113-8677, Japan*
[b]*Department of Pediatrics, Shimane University, Faculty of Medicine, Izumo, Shimane, Japan*
[c]*Department of Molecular Laboratory Medicine, Kyoto Prefectural University of Medicine Graduate School of Medical Science, Kyoto, Japan*
[d]*Department of Hematology/Oncology, Gunma Children's Medical Center, Shibukawa, Gunma, Japan*

Received 20 May 2007; accepted 25 September 2007

Abstract The prognosis of leukemia developed in Down syndrome (DS) patients has improved markedly. Most DS leukemia occurs before 3 years of age and is classified as acute megakaryocytic leukemia (AMKL). Mutations in the *GATA1* gene have been found in almost all DS patients with AMKL. In contrast, it has been shown that occurrence of DS acute myeloid leukemia (DS-AML) after 3 years of age may indicate a higher risk for a poor prognosis, but its frequency is very low. Age is one of the significant prognostic indicators in DS-AML. The prognostic factor of gene alterations has not been reported in older DS-AML patients. We here describe the case of a 7-year-old DS boy with AML-M2, who had no history of transient abnormal myelopoiesis or any clinical poor prognostic factors, such as high white blood cell counts or extramedullary infiltration. We molecularly analyzed the *GATA1*, *FLT3*, *MLL*-partial tandem duplication, *NRAS*, and *RUNX1* (previously *AML1*) genes and did not detect any alterations. The patient has lived for more than 5 years after treatment on the AML99-Down protocol in Japan. This suggests that a patient lacking these genes alterations might belong to a subgroup of older DS-AML patients with good prognosis. Accumulation of more data on older pediatric DS-AML patients is needed.

1. Introduction

Children with Down syndrome (DS) have a ~20-fold higher incidence of leukemia than do unaffected children. Most DS leukemia is diagnosed as acute megakaryocytic leukemia (AMKL), which occurs before 3 years of age, and the prognosis has markedly improved [1–3]. Infants with DS and transient abnormal myelopoiesis are at high risk for later development of AMKL, usually by 3 years of age. Recently, it has been reported that mutations of *GATA1* are present in virtually all cases of DS acute myeloid leukemia (DS-AML) [4,5]. The same mutations are seen in transient abnormal myelopoiesis cases as well [5]. Furthermore, in paired samples from transient abnormal myelopoiesis and AMKL in the same children, identical *GATA1* mutations were found [4–6], suggesting that DS with transient abnormal myelopoiesis and AMKL are within a biologically homogeneous group. *GATA1* mutation is a very early event in the development of DS-AMKL and in the process of multistep leukemogenesis [4,7].

On the other hand, DS-AML occurring after the age of 3 years may be completely different from that occurring before the age of 3 years, and may instead be biologically similar to de novo AML in non-DS patients. Multivariate analysis of data showed that children with DS aged ≥2 years at diagnosis had an increased risk of relapse after treatment [2]. There has been no good classification of DS-AML patients between the age of 2 and 4 years. Classification of the biological differences would probably be more useful than a better age cut.

* Corresponding author. Tel.: +81-3-3823-2101; fax: +81-3-3824-1552.
E-mail address: m.kawamura@cick.jp (M. Kawamura).

0165-4608/08/$ – see front matter
doi:10.1016/j.cancergencyto.2007.09.018

Here we describe the case of a 7-year-old boy with DS-AML who lacked mutations of *GATA1*, *FLT3*, *MLL*-partial tandem duplication (PTD), *NRAS*, and *RUNX1* (previously *AML1*) genes. The prognostic factors for DS-AML, particularly in older children, are still unknown. The present case supports the hypothesis that DS-AML patients who do not have alteration of these genes have a good prognosis.

2. Case report

A 7-year-old boy with DS presenting with a persistent fever was admitted to our hospital because of anemia and thrombocytopenia. On admission, he had a pale face and systemic petechiae and purpuras. No cervical lymphadenopathy or hepatomegaly was noted. Blood testing revealed a white blood cell count of 7,500/μL with 9% myeloblasts, 8% segmented neutrophils, 15% monocytes, 49% lymphocytes, and 6% blasts, a hemoglobin concentration of 6.1 g/dL, and a platelet count of 41.2×10^4/μL. Bone marrow examination revealed 66% blasts (Fig. 1a) with 39.2% monocytoid blasts and 18.8% myeloblastic cells with Auer bodies (Fig. 1b) and azurophilic granules. The diagnosis of AML-M2 was made according to the morphological and immunophenotypic criteria of the French–American–British (FAB) classification in combination with other laboratory data.

Even though the differential count showed a predominance of monocytic cells, myeloblasts (15.2%) and myeloblastic cells (18.8%) were 34% of total. These cells were positive for peroxidase staining (73.5%), and both nonspecific (5.8%) and specific (55%) esterase staining. Nonspecific esterase-positive cells were <20% among blasts, which matches the criteria of FAB-M2. Immunophenotypic analysis of CD45+ cells showed the presence of CD13 (56.8%), CD33 (86%), CD38 (95.2%), and HLA-DR (26.7%) antigens and the absence of CD34 (2.7%), CD11b (11.7%), and CD14 (0.6%). CD11b and CD14 presented on monocytes were negative in this patient. Cytogenetic analysis demonstrated the 47,XY,+21c karyotype in 20 bone marrow cells.

The serum and urine lysozyme level has been used as an aid in distinguishing AML with maturation (FAB-M2) from acute myelomonocytic leukemia (M4). In this patient, the count of monocytes in peripheral blood was 1,125/μL, which is less than the 5,000/μL of the FAB-M2 criteria. The serum lysozyme level was 25 μg/mL (normal range, 5–10 μg/mL) and the urine lysozyme level was 0 μg/mL. The level of lysozyme of this patient in peripheral blood was less than threefold of the normal range. Collectively, these data led us to diagnose this patient with AML-M2.

The patient was treated on the Japanese Childhood AML Cooperative Study Group Protocol for DS patients (AML99-Down protocol), which consists of pirarubicin (THP-ADR) (25 mg/m^2 on days 1 and 2), etoposide (150 mg/m^2 on days 3–5), and cytosine arabinoside (Ara-C) (100 mg/m^2 on days 1–7) at five cycles every month [8,9]. No prophylaxis for the central nervous system was performed.

On the first cycle of chemotherapy, he had severe mucositis and high fever for 5 weeks. On the second cycle, he had high fever during therapy. We considered this fever a side effect of Ara-C, and therefore methylprednisolone was given for 30 minutes prior to drip infusion of Ara-C. The patient obtained complete remission after the first cycle of chemotherapy and has continued in complete remission for 5 years without any reoccurrence.

3. Analysis of *GATA1*, *FLT3*, *MLL*, *NRAS*, and *RUNX1* genes

Written informed consent was obtained from the parents of the patient. RNA extracted from his bone marrow cells at

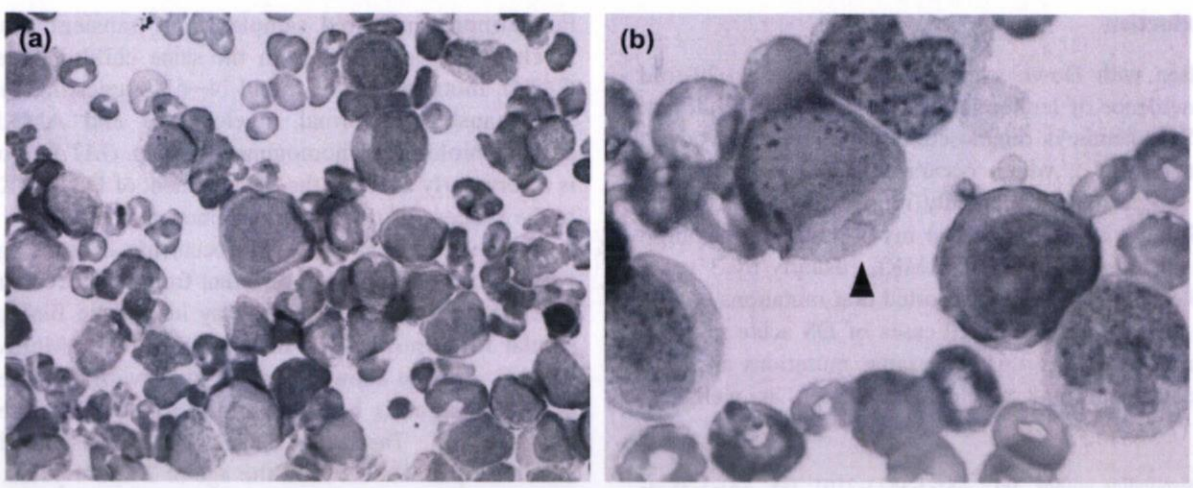

Fig. 1. Initial bone marrow smear at diagnosis. (a) Bone marrow aspirate showing hypercellularity (Giemsa staining). (b) Leukemic cells with Auer bodies (arrowhead).

diagnosis was reverse transcribed to cDNA and alterations of *GATA1*, *FLT3*, *MLL*-PTD, *NRAS*, and *RUNX1* genes were examined as previously described [10–13]. Briefly, mutational analysis of *GATA1* within exon 2, where there are hot spots, was performed with reverse transcription-polymerase chain reaction (RT-PCR) followed by direct sequencing [11]. Point mutations of *FLT3*-D835/I836 were examined with restriction fragment length polymorphism (RFLP)-PCR [12] and *FLT3*-internal tandem duplication (ITD) was analyzed with RT-PCR [11,13]. *MLL*-PTD was examined with simple first-round RT-PCR using the primer pair located between exon 9 and exon 4 [14]. Mutation of *NRAS* and *RUNX1* genes was examined with PCR-single strand conformation polymorphism analysis (SSCP) and direct sequencing [15].

4. Discussion

Lange et al. [16] studied 1,206 children with AML, including 118 (9.8%) DS patients. Among these, >95% of AML patients with DS were <5 years old. FAB-M7 (AMKL) was found in 62%, and FAB-M1or M2 in 10%. Children under 2 years ($n = 94$) treated on Children's Cancer Group (CCG) studies 2861 and 2891 had a 6-year EFS of 86%; those aged 2–4 years ($n = 58$), 70%; and those older than 4 years ($n = 9$), 28%. Outcome of children with DS-AML is excellent with standard induction therapy, but declines with increasing age; this report, however, gives no information about patients >4 years old [16].

Although white blood cell count at diagnosis is a significant predictor of outcome in non-DS AML, this is not the case for either DS or antecedent myelodysplastic syndrome patients. Extramedullary infiltration, which includes tumor nodules, skin infiltration, meningeal infiltration, gingival infiltration, or hepatosplenomegaly, has been discussed as a prognostic factor and is generally thought to indicate poor outcome in non-DS AML [8].

Monosomy 7 (−7) or deletion of the long arm of chromosome 7 [del (7q)] is found in only 4–5% of pediatric patients with AML. Although, cytogenetically, −7 is generally associated with a dismal prognosis in AML, even this may not be as unfavorable in those with DS [17]. Our patient did not have an acquired chromosomal abnormality in addition to trisomy 21 at diagnosis. Having no additional chromosomal abnormalities, including absence of −7, might be one of the good prognostic factors.

Our patient had no prior history of transient abnormal myelopoiesis or of the *GATA1* mutation in leukemic cells. In this respect, the leukemogenesis of this patient may differ from that typical of DS-AMKL patients <3 years old. DS-AMKL patients >3 years old at diagnosis often show the absence of a prior history of transient abnormal myelopoiesis. An age of >3 years at diagnosis may indicate only a different biological origin from those with a prior history of transient abnormal myelopoiesis and the *GATA1* mutation. In other words, there may be age-related biologic differences in the nature of AML in DS patients. We suggest that a better way to predict their prognosis would be by analyzing for the presence or absence of *GATA1* mutations and screening for the groups with good prognosis, rather than by the age at diagnosis, because the *GATA1* mutations are tightly associated with AMKL in DS patients, who are mostly younger children and have a good prognosis [1].

There is little clinical and genetic information on older pediatric patients with DS-AML with a poor prognosis. AML-M7 with *GATA1* mutations has a good prognosis among DS patients. This patient was 7 years old and his prognosis was good, suggesting that leukemogenesis in this case was not due to *GATA1* mutation.

DS-AML in older pediatric patients is considered to be similar to de novo non-DS AML. We therefore analyzed the same genetic prognostic factors in this patient as have been reported in de novo pediatric AML. There are no large studies of the genetic prognostic factors associated with older pediatric DS-AML, however, which made it difficult to compare the incidence of those mutations between non-DS AML and DS-AML among children. Particularly for older children with DS-AML, more accumulation of data is needed.

We examined ITD and D835/I836 mutations of *FLT3*. The prevalence and prognostic significance of these features are unknown in DS-AML. *FLT3*-ITD occurs in ~30% of adult AML patients and ~20% of pediatric AML patients [18–21]. *FLT3*-ITD is considered to predict poor prognosis in adult and pediatric AML patients [19,22–24]. On the other hand, ~10% of adult and pediatric AML patients have *FLT3*-D835/I836 mutations. AML patients with *FLT3*-D835/I836 mutations tend to have a poor prognosis as adults, but not as children [25,26]. Alterations of *FLT3* were not detected in the present patient. Given that this case was considered to be the same as de novo AML in a non-DS patient, the absence of *FLT3* alterations suggests a good prognosis.

We analyzed other possible prognostic factors, such as *MLL*-PTD, *NRAS*, and *RUNX1* mutations. *MLL*-PTD was detected in ~10% of AML patients with normal karyotype and in 90% of AML patients exhibiting trisomy 11 as the sole chromosome abnormality. The *MLL*-PTD was reported to be a subgroup of patients with an unfavorable prognosis in adult AML [14]. In a study of the Japanese Childhood AML Cooperative study group, AML patients with *MLL*-PTD comprised 13.3% and correlated with poor prognosis [21]. The prognostic impact of *NRAS* mutations, reported in 11–30% of AML patients, is still under discussion [27,28]. As for *RUNX1* mutation, we have reported that the mutations in pediatric hematologic malignancies are infrequent, but may be related to AML-M0, acquired trisomy 21, and leukemic transformation [10]. Furthermore, non-constitutional chromosome 21 in the leukemic clone may also lead to an unfavorable prognosis. No mutations of these genes were found in our patient, suggesting a good prognosis.

Table 1
Frequency of Down syndrome acute myeloid leukemia and myelodysplastic syndrome patients in published studies, including pediatric patients older than 4 years

Study group	Accrual period, mo/yr	DS-AML/AML patients, no./no. (%)	DS-AML patients >4 yr old, no.	References
POG8498	July 1984–July 1989	12/285 (4.2)	0	Ravindranath et al., 1992 [29]
Nagoya	Sept. 1986–Aug. 1992	9/NI	0	Kojima et al., 2000 [1]
NOPHO84/NOPHO88	July 1984–Dec. 1992	23/223 (10.3)	2	Lie et al., 1996 [30]
BFM 87/BFM 93	July 1987–Dec. 1994	40/633 (6.3)	3	Creutzig et al., 1996 [31]
CCG 2861/2891	Mar. 1988–Oct. 1995	118/1206 (9.8)	3	Lange et al., 1998 [16]
Japan AT group/Down	Sept. 1987–Aug. 1997	33/NI	0	Kojima et al., 2000 [1]
CCG 2891	Oct. 1989–Oct. 1999	161/1108 (14.5)	9[a]	Gamis et al., 2003 [2]
AML99	Jan. 2000–Dec. /2003	66/418 (15.8)	2	Kobayashi et al., 2006 [8]

Abbreviations: DS-AML/MDS, Down syndrome acute myeloid leukemia and myelodysplastic syndrome; NI, no information.
[a] Nine patients are older than 5 years; data are shown separately for patients aged 2–5 years and older than 5 years.

Table 1 presents the frequency of DS-AML/MDS in children >4 years old from previous reports [1,2,8,16,29–31]. In BFM 87/BFM93, there were three such patients among 40 patients with DS-AML [31]. These three patients were 12, 15, and 16 years old at diagnosis, their FAB classification was M0, M2, and M4, and their white blood cell count at diagnosis was 2,600/μL, 22,600/μL, and 1,400/μL, respectively. The 12-year-old girl died from sepsis after four weeks of consolidation therapy; the other two patients were not treated [31]. In the CCG-2861 and CCG-2891 studies, three patients were reported to be >5 years old [16], two of whom died of disease and one from toxicity. On the AML99-Down protocol, there were two patients >4 years old (one being the present patient) [8]. A 4-year-old boy with AML FAB-M5a who failed to obtain complete remission after two courses of induction therapy and received cord blood stem cell transplantation was, at writing, still alive [32].

To date, there are only a few individual case reports of children >4 years old [32,33]. For DS patients, immunologic disorders, congenital heart disease, and other factors possibly caused disease-related and treatment-related mortality. Considering the high incidence of therapy-related mortality, overtreatment should be avoided.

No alterations in *GATA1*, *FLT3*, *MLL*-PTD, *NRAS*, or *RUNX1* were found in our patient, suggesting that he belongs to a subgroup, among older DS-AML patients, with good prognosis. Because the prognostic factors for DS-AML are still unknown, particularly in older children, further data accumulation is needed.

Acknowledgments

Gracious thanks are due to Janet E. Lewis of the University of Wisconsin–Madison for preparing the manuscript.

References

[1] Kojima S, Sako M, Kato K, Hosoi G, Sato T, Ohara A, Koike K, Okimoto Y, Nishimura S, Akiyama Y, Yoshikawa T, Ishii E, Okamura J, Yazaki M, Hayashi Y, Eguchi M, Tsukimoto I, Ueda K. An effective chemotherapeutic regimen for acute myeloid leukemia and myelodysplastic syndrome in children with Down's syndrome. Leukemia 2000;14:786–91.

[2] Gamis AS, Woods WG, Alonzo TA, Buxton A, Lange B, Barnard DR, Gold S, Smith FO. Children's Cancer Group Study 2891. Increased age at diagnosis has a significantly negative effect on outcome in children with Down syndrome and acute myeloid leukemia: a report from the Children's Cancer Group Study 2891. J Clin Oncol 2003;21:3415–22.

[3] Fong CT, Brodeur GM. Down's syndrome and leukemia: epidemiology, genetics, cytogenetics and mechanisms of leukemogenesis. Cancer Genet Cytogenet 1987;28:55–76.

[4] Wechsler J, Greene M, McDevitt MA, Anastasi J, Karp JE, Le Beau MM, Crispino JD. Acquired mutations in *GATA1* in the megakaryoblastic leukemia of Down syndrome. Nat Genet 2002;32:148–52.

[5] Hitzler JK, Cheung J, Li Y, Scherer SW, Zipursky A. *GATA1* mutations in transient leukemia and acute megakaryoblastic leukemia of Down syndrome. Blood 2003;101:4301–4.

[6] Groet J, McElwaine S, Spinelli M, Rinaldi A, Burtscher I, Mulligan C, Mensah A, Cavani S, Dagna-Bricarelli F, Basso G, Cotter FE, Nizetic D. Acquired mutations in *GATA1* in neonates with Down's syndrome with transient myeloid disorder. Lancet 2003;361:1617–20.

[7] Shimada A, Xu G, Toki T, Kimura H, Hayashi Y, Ito E. Fetal origin of the *GATA1* mutation in identical twins with transient myeloproliferative disorder and acute megakaryoblastic leukemia accompanying Down syndrome. Blood 2004;103:366.

[8] Kobayashi R, Tawa A, Hanada R, Horibe K, Tsuchida M, Tsukimoto I. Japanese childhood AML cooperative study group. Extramedullary infiltration at diagnosis and prognosis in children with acute myelogenous leukemia. Pediatr Blood Cancer 2007;48:392–8.

[9] Tsukimoto I, Tawa A, Hanada R, Tabuchi K, Kigasawa H, Tsuchiya S, Tsuchida M, Yabe H, Nakayama H, Kudo K, Kobayashi R, Hamamoto K, Imaizumi M, Morimoto M, Horibe K. Excellent outcome of risk stratified treatment for childhood acute myeloid leukemia-AML99 trial [Abstract]. Blood 2005;106:889.

[10] Taketani T, Taki T, Takita J, Tsuchida M, Hanada R, Hongo T, Kaneko T, Manabe A, Ida K, Hayashi Y. *AML1/RUNX1* mutations are infrequent, but related to AML-M0, acquired trisomy 21, and leukemic transformation in pediatric hematologic malignancies. Genes Chromosomes Cancer 2003;38:1–7.

[11] Xu G, Nagano M, Kanezaki R, Toki T, Hayashi Y, Taketani T, Taki T, Mitui T, Koike K, Kato K, Imaizumi M, Sekine I, Ikeda Y, Hanada R, Sako M, Kudo K, Kojima S, Ohneda O, Yamamoto M, Ito E. Frequent mutations in the *GATA-1* gene in the transient myeloproliferative disorder of Down syndrome. Blood 2003;102:2960–8.

[12] Taketani T, Taki T, Sugita K, Furuichi Y, Ishii E, Hanada R, Tsuchida M, Ida K, Hayashi Y. *FLT3* mutations in the activation loop

of tyrosine kinase domain are frequently found in infant ALL with *MLL* rearrangements and pediatric ALL with hyperdiploidy. Blood 2004;103:1085–8.

[13] Shimada A, Taki T, Tabuchi K, Tawa A, Horibe K, Tsuchida M, Hanada R, Tsukimoto I, Hayashi Y. *KIT* mutations, and not *FLT3* internal tandem duplication, are strongly associated with a poor prognosis in pediatric acute myeloid leukemia with t(8;21): a study of the Japanese Childhood AML Cooperative Study Group. Blood 2006;107:1806–9.

[14] Schnittger S, Kinkelin U, Schoch C, Heinecke A, Haase D, Haferlach T, Büchner T, Wörmann B, Hiddemann W, Griesinger F. Screening for MLL tandem duplication in 387 unselected patients with AML identify a prognostically unfavorable subset of AML. Leukemia 2000;14:796–804.

[15] Sheng XM, Kawamura M, Ohnishi H, Ida K, Hanada R, Kojima S, Kobayashi M, Bessho F, Yanagisawa M, Hayashi Y. Mutations of the *RAS* genes in childhood acute myeloid leukemia, myelodysplastic syndrome and juvenile chronic myelocytic leukemia. Leuk Res 1997;21:697–701.

[16] Lange BJ, Kobrinsky N, Barnard DR, Arthur DC, Buckley JD, Howells WB, Gold S, Sanders J, Neudorf S, Smith FO, Woods WG. Distinctive demography, biology, and outcome of acute myeloid leukemia and myelodysplastic syndrome in children with Down syndrome: Children's Cancer Group Studies 2861 and 2891. Blood 1998;91:608–15.

[17] Bunin N, Nowell PC, Belasco J, Shah N, Willoughby M, Farber PA, Lange B. Chromosome 7 abnormalities in children with Down syndrome and preleukemia. Cancer Genet Cytogenet 1991;54: 119–26.

[18] Meshinchi S, Stirewalt DL, Alonzo TA, Zhang Q, Sweetser DA, Woods WG, Bernstein ID, Arceci RJ, Radich JP. Activating mutations of RTK/ras signal transduction pathway in pediatric acute myeloid leukemia. Blood 2003;102:1474–9.

[19] Zwaan CM, Meshinchi S, Radich JP, Veerman AJ, Huismans DR, Munske L, Podleschny M, Hahlen K, Pieters R, Zimmermann M, Reinhardt D, Harbott J, Creutzig U, Kaspers GJ, Griesinger F. *FLT3* internal tandem duplication in 234 children with acute myeloid leukemia: prognostic significance and relation to cellular drug resistance. Blood 2003;102:2387–94.

[20] Liang DC, Shih LY, Hung IJ, Yang CP, Chen SH, Jaing TH, Liu HC, Wang LY, Chang WH. *FLT3*–TKD mutation in childhood acute myeloid leukemia. Leukemia 2003;17:883–6.

[21] Shimada A, Taki T, Tabuchi K, Taketani T, Hanada R, Tawa A, Tsuchida M, Horibe K, Tsukimoto I, Hayashi Y. Japanese Childhood AML Cooperative Study Group. Tandem duplications of *MLL* and *FLT3* are correlated with poor prognoses in pediatric acute myeloid leukemia: a study of the Japanese childhood AML Cooperative Study Group (Epub ahead of print: Aug. 30, 2007). Pediatr Blood Cancer 2007.

[22] Yokota S, Kiyoi H, Nakao M, Iwai T, Misawa S, Okuda T, Sonoda Y, Abe T, Kahsima K, Matsuo Y, Naoe T. Internal tandem duplication of the *FLT3* gene is preferentially seen in acute myeloid leukemia and myelodysplastic syndrome among various hematological malignancies: a study on a large series of patients and cell lines. Leukemia 1997;11:1605–9.

[23] Kottaridis PD, Gale RE, Langabeer SE, Frew ME, Bowen DT, Linch DC. Studies of *FLT3* mutations in paired presentation and relapse samples from patients with acute myeloid leukemia: implications for the role of *FLT3* mutations in leukemogenesis, minimal residual disease detection, and possible therapy with FLT3 inhibitors. Blood 2002;100:2393–8.

[24] Abu-Duhier FM, Goodeve AC, Wilson GA, Gari MA, Peake IR, Rees DC, Vandenberghe EA, Winship PR, Reilly JT. *FLT3* internal tandem duplication mutations in adult acute myeloid leukaemia define a high-risk group. Br J Haematol 2000;111:190–5.

[25] Yamamoto Y, Kiyoi H, Nakano Y, Suzuki R, Kodera Y, Miyawaki S, Asou N, Kuriyama K, Yagasaki F, Shimazaki C, Akiyama H, Saito K, Nishimura M, Motoji T, Shinagawa K, Takeshita A, Saito H, Ueda R, Ohno R, Naoe T. Activating mutation of D835 within the activation loop of FLT3 in human hematologic malignancies. Blood 2001;97: 2434–9.

[26] Thiede C, Steudel C, Mohr B, Schaich M, Schakel U, Platzbecker U, Wermke M, Bornhauser M, Ritter M, Neubauer A, Ehninger G, Illmer T. Analysis of FLT3-activating mutations in 979 patients with acute myelogenous leukemia: association with FAB subtypes and identification of subgroups with poor prognosis. Blood 2002;99: 4326–35.

[27] Bacher U, Haferlach T, Schoch C, Kern W, Schnittger S. Implications of *NRAS* mutations in AML: a study of 2502 patients. Blood 2006;107:3847–53.

[28] Kiyoi H, Naoe T, Nakano Y, Yokota S, Minami S, Miyawaki S, Asou N, Kuriyama K, Jinnai I, Shimazaki C, Akiyama H, Saito K, Oh H, Motoji T, Omoto E, Saito H, Ohno R, Ueda R. Prognostic implication of *FLT3* and *N-RAS* gene mutations in acute myeloid leukemia. Blood 1999;93:3074–80.

[29] Ravindranath Y, Abella E, Krischer JP, Wiley J, Inoue S, Harris M, Chauvenet A, Alvarado CS, Dubowy R, Ritchey AK, Land V, Steuber CP, Weinstein H. Acute myeloid leukemia (AML) in Down's syndrome is highly responsive to chemotherapy: experience on Pediatric Oncology Group AML Study 8498. Blood 1992;80:2210–4.

[30] Lie SO, Jonmundsson G, Mellander L, Siimes MA, Yssing M, Gustafsson G. A population-based study of 272 children with acute myeloid leukaemia treated on two consecutive protocols with different intensity: best outcome in girls, infants, and children with Down's syndrome. Nordic Society of Paediatric Haematology and Oncology (NOPHO). Br J Haematol 1996;94:82–8.

[31] Creutzig U, Ritter J, Vormoor J, Ludwig WD, Niemeyer C, Reinisch I, Stollmann-Gibbels B, Zimmermann M, Harbott J. Myelodysplasia and acute myelogenous leukemia in Down's syndrome: a report of 40 children of the AML-BFM Study Group. Leukemia 1996;10:1677–86.

[32] Kurosawa H, Tsuboi T, Shimaoka H, Okuya M, Nakajima D, Matsunaga T, Hagisawa S, Sato Y, Sugita K, Eguchi M. Long-term remission in an acute monoblastic leukemia patient with Down syndrome after cord blood transplantation [In Japanese]. Rinsho Ketsueki 2005;46:274–7.

[33] Yamaguchi Y, Fujii H, Kazama H, Iinuma K, Shinomiya N, Aoki T. Acute myeloblastic leukemia associated with trisomy 8 and translocation 8;21 in a child with Down syndrome. Cancer Genet Cytogenet 1997;97:32–4.

Pediatr Blood Cancer 2008;50:213–217

Expression of KIT and PDGFR Is Associated With a Good Prognosis in Neuroblastoma

Akira Shimada, MD,[1] Junko Hirato, MD,[2] Minoru Kuroiwa, MD,[3] Akira Kikuchi, MD,[4] Ryoji Hanada, MD,[4] Kimiko Wakai, CT,[5] and Yasuhide Hayashi, MD[1]*

Background. The clinical outcome of neuroblastoma (NB) depends on age, stage, and *MYCN* amplification. Receptor tyrosine kinases (RTKs) promote cell growth, migration, and metastasis in cancer cells, including NB. However, the correlation of the expression profile of RTKs with prognosis in NB remains controversial. ***Procedure.*** Expression and mutation analysis of *KIT*, *PDGFR*, *FLT3*, *RET*, and *TRKA* mRNAs were performed in 24 NB cell lines and 40 tumor samples using RT-PCR followed by direct sequencing. Immunohistochemical analysis of KIT and PDGFR protein expression was also examined in 38 paraffin sections of NB tumor samples. ***Results.*** The expression of *KIT*, *PDGFRβ*, and *FLT3* mRNA was associated with NB in patients under 1 year ($P < 0.02$) and *TRKA* expression ($P < 0.001$). The loss of expression of these kinases was associated with *MYCN* amplification ($P < 0.02$) and advanced stages of disease in patients over 1 year of age ($P < 0.005$). *PDGFRα* mRNA expression was detected in all cell lines and tumor samples, and *RET* mRNA expression was not associated with any clinical parameters. Immunohistochemistry results showed the similar findings. We did not find any activating mutations in *KIT*, *PDGFR*, *FLT3*, or *RET*. Notably, the GNNK$^-$ isoform of *KIT* was predominant in all cell lines and clinical samples. ***Conclusion.*** Expression of *KIT*, *PDGFRβ*, and *FLT3* was associated with a good prognosis in NB. The loss of expression of these RTKs might correlate to the disease progression of NB. Pediatr Blood Cancer 2008;50:213–217.

Key words: *FLT3*; *KIT*; neuroblastoma; *PDGFR*; receptor tyrosine kinase

INTRODUCTION

The receptor tyrosine kinases (RTKs) play an important role in the growth, migration, metastasis and angiogenesis in varieties of malignancies [1–3]. KIT is one of the type III RTKs and is well known to have roles not only in hematopoiesis, but also in germ cell and melanocyte development and differentiation as well as in neuroectodermal tumor cells [1–9]. Recently, KIT expression in NB has been reported to be associated with a poor prognosis with MYCN amplification [4,9]. On the other hand, another report suggested that KIT expression was associated with a good prognosis [7]. Moreover, a tyrosine kinase inhibitor, imatinib, has been shown to have an inhibitory effect for NB cell growth in vitro and in vivo [4–6]; however, imatinib was suggested not to inhibit the stem cell factor (SCF)/KIT pathway in NB cells [6]. Therefore, the therapeutic mechanism of imatinib in NB remains undetermined. *KIT* mutations have been frequently found in gastrointestinal stromal tumor (GIST) [10] and a subtype of acute myeloid leukemia (AML) [11], but not in NB [8]. The platelet derived growth factor receptor (PDGFR)-α has important roles in the development of neural crest-derived cells [12]. *PDGFRα* mutation has been frequently found in GIST [13]. PDGFRβ is overexpressed in metastatic medulloblastoma, and has been considered to have a more oncogenic potential than *PDGFRα* [14]. The roles of *PDGFRα* and *PDGFRβ* remain to be elucidated in NB.

FLT3 and RET have been reported to have roles in proliferation and differentiation in NB [15,16]. Although *FLT3*-internal tandem duplication (ITD) is a poor prognostic factor in AML [17], *FLT3*-ITD or kinase domain mutations have not yet been reported in NB. The RET receptor signal pathway is functional in most NB [16,18]. *RET* gene mutations have been identified in multiple endocrine tumors [19]. The expression of TRKA has been associated with good clinical outcome in NB. On the other hand, Tacconelli et al. [20] reported that the alternative spliced isoform III of TRKA has oncogenic potential. Therefore, we performed expression and mutation analysis of these 5 RTK (*KIT*, *PDGFRs*, *FLT3*, *RET*, and *TRKA*) genes in 24 NB cell lines and 40 clinical specimens.

Here we described that the expression of *KIT*, *PDGFRβ*, and *FLT3* is associated with NB in patients under 1 year of age and with a good prognosis. The loss of expression of these RTKs may be associated with NB disease progression.

MATERIALS AND METHODS

Cell Lines and Clinical Samples

Twenty-four NB cell lines were examined in this study (Supplemental Table I). RNAs were extracted from 40 frozen tumor samples using a QIAGEN RNA extraction kit (Qiagen, Chatsworth, CA), which were obtained before chemotherapy from January 2001 to December 2005. Twenty of these samples were taken from patients under 1 of age, and they received surgical resection and chemotherapy. All patients except for one are alive. Five patients were stages I or II and over 1 year of age and received surgical resection and chemotherapy and were alive. Fifteen patients had advanced stage and were over 1 year of age; they received surgical resection, radiation therapy, and intensive chemotherapy including autologous-SCT [21] (Table I); however, five patients (33.3%) died due to the disease progression after autologous-SCT. Informed consent was obtained from parents. The institutional review board of Gunma Children's Medical Center approved this project.

This article contains Supplementary Material available at http://www.interscience.wiley.com/jpages/1545-5009/suppmat.

[1]Department of Hematology/Oncology, Gunma Children's Medical Center, Gunma, Japan; [2]Department of Human Pathology, Gunma University Graduate School of Medicine, Gunma, Japan; [3]Department of Pediatric Surgery, Gunma Children's Medical Center, Gunma, Japan; [4]Department of Hematology/Oncology, Saitama Children's Medical Center, Saitama, Japan; [5]Department of Clinical laboratory, Gunma Children's Medical Center, Gunma, Japan

Grant sponsor: Ministry of Health, Labor, and Welfare of Japan.

*Correspondence to: Yasuhide Hayashi, Director, Gunma Children's Medical Center, 779, Shimohakoda, Hokkitsu, Shibukawa, Gunma 377-8577, Japan. E-mail: hayashiy-tky@umin.ac.jp

Received 18 August 2006; Accepted 16 May 2007

DOI 10.1002/pbc.21288

TABLE I. Expression of *KIT, PDGFRβ, FLT3, RET* in 40 Clinical NB Samples by RT-PCR

	No. of patients	*KIT* (%)	*PDGFRβ* (%)	*FLT3* (%)	*RET* (%)
Age					
<1 year	20	20 (100)	19 (95)	19 (95)	8 (40)
>1 year	20	12 (60)	10 (50)	13 (65)	9 (45)
		($P = 0.0016$)	($P = 0.0014$)	($P = 0.0177$)	ns
MYCN status					
>5 copies	6	2 (33.3)	2 (33.3)	2 (33.3)	1 (16.7)
1 copy	34	30 (88.2)	27 (79.4)	30 (88.2)	16 (47.1)
		($P = 0.0006$)	($P = 0.0198$)	($P = 0.0019$)	ns
Clinical stage					
III, IV, and over 1 year old	15	7 (46.7)	7 (46.7)	8 (53.3)	4 (26.7)
I, II, IVs at any age	25	25 (100)	22 (88)	24 (96)	13 (52)
		($P < 0.0001$)	($P = 0.0046$)	($P = 0.0011$)	ns
TRKA					
Positive	28	27 (96.4)	25 (89.3)	27 (96.4)	12 (42.9)
Negative	12	5 (41.7)	4 (33.3)	5 (41.7)	5 (41.7)
		($P < 0.0001$)	($P = 0.0003$)	($P < 0.0001$)	ns
Total	40	32 (80)	29 (72.5)	32 (80)	17 (42.5)

P-value is analyzed for the correlation between RTK expression and age, *MYCN* amplification, clinical stage, and TRKA expression, respectively. ns represents not significant.

Expression and Mutation Analysis of *KIT* and *PDGFR*

The procedure was reported previously. Briefly, a total of 4 μg of RNA was reverse transcribed to cDNA. Using 1 μl of the cDNA, polymerase chain reaction (PCR) was performed using primer pairs for extracellular (EC), juxtamembrane (JM), transmembrane (TM), and the second tyrosine kinase (TK2) domains of *KIT* and *PDGFR* using an ABI 2700 thermal cycler (Applied Biosystems, Tokyo, Japan; Supplemental Table II) [11,22]. If the PCR-product was found as the estimated size and confirmed by sequencing directly, we evaluated it as positive expression of mRNA.

Mutation analyses of *KIT* and *PDGFR* in 24 NB cell lines were performed by direct sequencing using an ABI prism 310 sequence analyzer (Applied Biosystems). The mRNA expression of each ligand (*SCF, PDGFA*, and *PDGFB*) was also analyzed by RT-PCR.

Expression and Mutation Analysis of *FLT3*

Using 1 μl of the cDNA, PCR amplification was performed for the JM or TK2 domain of the *FLT3* gene. The PCR procedure has been reported previously using primer pairs R5, R6 and 17F, TKR [23]. If more than two bands were found, the amplified products were cut from the gel, purified with a QIAquick gel extraction kit (Qiagen) and directly sequenced.

Expression and Mutation Analysis of *RET*

Using 1 μl of the cDNA, PCR amplification was performed for the TM and TK domain of the *RET* gene. PCR was performed using previously reported condition and primer pairs RET-TM(+) and RET-TK2(−) [24]. *RET* isoforms, RET9 and RET51, were analyzed as previously reported [25].

Expression and Mutation Analysis of *TRKA*

TRKA mRNA expression was analyzed using newly designed primer pairs, TRKA-F and TRKA-R (Supplemental Table II). This primer pair could distinguish the alternative spliced form I (deleted exon 9), II (no-deletion), and III (exons 6, 7, and 9) [24] by the forward primer in exon 5 and reverse primer in exon 10.

Protein Expression Analysis

Paraffin sections were obtained from 38 NB samples (Table II). Eight samples were classified as advanced stage and older than 1 year old. Ten RNAs and ten paraffin sections were obtained from the same patients. The expression of KIT, PDGFRα and PDGFRβ proteins was analyzed using the avidin–biotin–peroxidase complex method on paraffin sections [26]. Antibodies of KIT (DAKO, A4502, diluted 1:80), PDGFRα (SantaCruz, CA, USA, sc-338,

TABLE II. Expression of KIT and PDGFRβ in NB Tumor Specimens by Immunohistochemistry

	Number of patients	KIT (%)	PDGFRβ (%)
Age			
<1 year	27	20 (74)	20 (74)
>1 year	11	3 (27.3)	4 (36.4)
		($P = 0.0074$)	($P = 0.019$)
MYCN status			
>5 copies	6	1 (16.2)	0
1 copy	32	22 (68.8)	24 (75)
		($P = 0.017$)	($P = 0.0052$)
Clinical stage			
III, IV, and over 1 year old	8	2 (25)	1 (12.5)
I, II, IVs in any age	30	21 (70)	22 (73.3)
		($P = 0.014$)	($P = 0.0011$)
Shimada's Histology			
Favorable	27	19 (70.4)	21 (77.8)
Unfavorable	11	4 (36.4)	3 (27.3)
		($P = 0.052$)	($P = 0.0021$)
Total	38	23 (60.5)	24 (63.2)

P-value is analyzed for the correlation between each RTK expression and age, *MYCN* gene amplification, clinical stages, and histology.

diluted 1:200) and PDGFRβ (SantaCruz, sc-6252, diluted 1:200) were used. We also analyzed the expression of KIT and PDGFRβ in 6 ganglioneuroma samples (Table III). GIST specimens were used for the positive controls. The evaluation of immunohistochemistry was performed by two independent observers (AS and JH). We evaluated the complete cytoplasm and membrane staining in more than 30% of cells as positive, and cytoplasm or membrane staining in less than 30% of cells as negative. We considered that the positive specimens showed the expression of the protein.

Statistical Analysis

Statistical analysis was performed using Statview software (SAS). The χ^2-test was used to correlate the categorical variables. The prognostic significance of the clinical variables was assessed by using Cox proportional hazards model. For all analyses, the *P* values were 2-tailed, and a *P*-value of less than 0.05 was considered statistically significant.

RESULTS

Expression and Mutation Analysis of *KIT*

KIT mRNA expression was found in 22 (91.7%) of 24 cell lines with RT-PCR (Supplemental Table I). All cell lines predominantly showed a 12 bp (GGTAACAACAAA) deleted product ($GNNK^-$ isoform) at the end of the extra cellular domain (exon 9) compared to the wild-type of *KIT* (Supplemental Fig. 1) [27]. We could not find any activating mutations as previously reported in GIST and AML [10,11]. Two single nucleotide polymorphisms (SNPs) were found [541aa, A > C of 1642 bp in exon 10 (Reference SNP (refSNP) Cluster Report: rs 3822214 by NCBI) in SCMC-N4 and SKNSH, 862aa, G > C of 2,607 bp in exon 18 (rs 3733542) in SJNB-5 and SKNSH]. A silent mutation was also found (I798I, ATC > ATT of 2,414 bp in exon 17 in SJNB-8). All cell lines, except for one, expressed *SCF*. Both soluble and membranous bound forms of *KIT* mRNA were found.

KIT expression was detected in 32 (80.0%) of 40 tumor samples by RT-PCR (Table I) and 23 (60.5%) of 38 paraffin sections of tumor samples by immunohistochemistry (Table II). The expression of mRNA and protein was measured in ten patients using both RT-PCR and immunohistochemistry. The expression of *KIT* mRNA and protein was associated with NB patients under 1 year ($P = 0.0016$, 0.0074, respectively) and inversely associated with *MYCN* amplification ($P = 0.0006$, 0.017, respectively) and Stages 3 or 4 NB patients over 1 year old ($P < 0.0001$, 0.014, respectively). *KIT* mRNA expression was significantly associated with *TRKA* mRNA expression ($P < 0.001$). Multivariate analysis showed the coefficient of correlation between *KIT* mRNA and *TRKA* mRNA was 0.627 (0.398–0.785, $P < 0.001$) and between KIT mRNA and survival was 0.665 (0.446–0.809, $P < 0.001$). The KIT protein expression was found in two of four differentiating NB samples and five of six samples of ganglioneuroma (Table III). The difference of expression rate of KIT protein between neuroblastoma (NB) and ganglioneuroma or between differentiating and poorly differentiated NB were not statistically significant.

Expression and Mutation Analysis of *PDGFRs*

PDGFRα mRNA was detected in all cell lines and tumor samples by RT-PCR (Supplemental Table I). As for the mutation of *PDGFRα*, no activating mutations were found. Three SNPs were found (567aa A > G of 1,849 bp in exon12 (rs 1873778) in SJNB4, 603aa G > A of 1957 bp in exon13 (rs 10028020) in SJNB4, NB16, NB69, LAN2, and SKNSH, 824aa C > T of 2,620 bp in exon 18 (rs 2228230) in SJNB-5, SJNB-8, NB-19, LAN-1, LAN-5, and SKNSH). Silent mutation was found in GOTO (V533V, GTG > GTA of 1,747 bp in exon 11). PDGFRα protein was strongly expressed in almost all tumor samples by immunohistochemistry.

PDGFRβ mRNA was expressed in 14 (58%) of 24 cell lines and 29 (73%) of 40 NB samples using RT-PCR (Tables I and II). *PDGFRβ* was expressed in 24 (63%) of 38 tumor samples by immunohistochemistry (Table III). The expression of *PDGFRβ* mRNA and protein was associated with NB patients under 1 year ($P = 0.0014$ and 0.019, respectively) and inversely associated with *MYCN* amplification ($P = 0.0198$ and 0.0052, respectively), advanced stage patients one year old and over ($P = 0.0046$ and 0.0011, respectively). The correlation between *PDGFRβ* and *TRKA* mRNA expression was significant ($P = 0.0003$). Multivariate analysis showed the coefficient of correlation between *PDGFRβ* mRNA and *TRKA* mRNA was 0.574 (0.320–0.751, $P < 0.001$) and between *PDGFRβ* mRNA and survival was 0.525 (0.256–0.719, $P = 0.004$). The correlation between PDGFRβ protein expression and a favorable histology was also significant ($P = 0.0021$). The

TABLE III. Correlation of KIT and PDGFRβ Expression to Histopathology of NB According to INPC System

INPC system	Number of patients	KIT (%)	PDGFRβ (%)
Neuroblastoma (Schwannian stroma-poor)			
Undifferentiated	1	0	0
Differentiating	4	2 (50)	4 (100)
Poorly differentiated	27	17 (63)	16 (59.3)
Ganglioneuroblastoma			
Intermixed (Schwannian stroma-rich)	4	2 (50)	4 (100)
Nodular	2	2 (100)	1 (50)
Total	38	23 (60.5)	25 (65.8)
Ganglioneuroma (Schwannian stroma-dominant)	6	5 (83.3)	6 (100)

The difference of expression rate of KIT or PDGFRβ protein between neuroblastoma and ganglioneuroma was not statistically significant. The difference of expression rate of KIT or PDGFRβ protein between differentiating and poorly differentiated neuroblast.

expression of PDGFRβ was found in all four differentiating NB samples and all five ganglineuroblastoma samples (Table III). The difference of expression rate of PDGFRβ protein between NB and ganglioneuroma or between differentiating and poorly differentiated NB were not statistically significant.

Expression and Mutation Analysis of *FLT3*

FLT3 mRNA expression was detected in 19 (79.2%) of 24 cell lines and in 32 (80%) of 40 tumor samples by RT-PCR (Table I and Supplemental Table I). No ITDs or kinase domain mutations were observed in any cell lines. *FLT3* expression was associated with NB patients under 1 year ($P = 0.0177$) and *TRKA* expression ($P < 0.0001$; Table I). Inverse correlations were observed for *MYCN* amplification ($P = 0.0019$) and advanced stage patients over one year old ($P = 0.0011$). FLT3 protein expression was not examined.

Expression and Mutation Analysis of *RET*

RET expression was detected in 22 (91.6%) of 24 cell lines and in 17 (42.5%) of 40 tumor samples by RT-PCR (Table I and Supplemental Table I). However, no mutations were found in this study. We identified SNPs (691aa or 769aa) of the *RET* gene. *RET* expression was not associated with any clinical findings (Table I). Furthermore, we examined the expression of both isoforms RET51 and RET9. There were no correlations between the RET isoforms and the clinical findings.

Expression and Mutation Analysis of *TRKA*

TRKA expression was detected in 7 (29.2%) of 24 cell lines and in 28 (70.0%) of 40 tumor samples by RT-PCR (Table I and Supplemental Table I). *TRKA* expression was associated with NB in patients under age 1 year ($P = 0.0006$) and with good prognosis (Table I). We examined the expression of the TRKA isoform, but did not detect isoform III in any cell lines or tumor samples [20]. On the other hand, we found another novel isoform (deletion of exons 7–9) in 6 (25%) in 24 cell lines (SJNB-2, SJNB-6, NB1, TGW, SKNSH, SCMC-N4) with the coexpression of isoforms I or II, which we referred to as isoform IV in this article (Supplemental Fig. 2). However, we could not find this isoform IV in any of 40 tumor samples.

DISCUSSION

The aberrant expression of KIT and SCF has been reported in several solid tumors, such as small cell lung cancer [28], gynecological tumors [29], and breast cancer [30]. However, *KIT* mutations are rarely reported in other cancers [31–33] except for GIST [10] and the core-binding factor AML [11]. An autocrine or paracrine loop of KIT and SCF has been hypothesized in NB cell proliferation [34]. Moreover, the $GNNK^-$ isoform of *KIT* has been shown to be predominantly expressed in varieties of tumors, such as AML and germ cell tumor [35,36], and the $GNNK^-$ isoform has a growth advantage compared with the $GNNK^+$ isoform and phosphorylates downstream signals, such as MAP and STAT kinases [27]. In this study, KIT expression was associated with NB patients under 1 year of age and good prognosis as previously reported [7]. The $GNNK^-$ isoform was predominantly expressed in NB patients. An inverse correlation between KIT expression and *MYCN* amplification was observed and it supported the observation of Krams et al. [7]. On the other hand, KIT expression has been reported to be associated with a poor prognosis and with *MYCN* amplification in NB [4,9]. These different results may due to the differences of experimental method, race or the number of patients analyzed. Moreover, the loss of KIT expression has also been reported in advanced cancer, including breast cancer [32], melanoma [37], thyroid cancer [38], and ovarian cancer [39]. The loss of KIT expression may be associated with NB tumor progression.

PDGFRs and their ligands, PDGFA and PDGFB, have an important role not only in embryogenesis, but also in the progression of some tumors, suggesting the presence of an autocrine or paracrine mechanism [40,41]. PDGFRs can become potent oncoproteins when they are overexpressed or mutated [40–42]. The intensive expression of PDGFRα protein was detected in this study, suggesting that expressed PDGFRα may be the therapeutic target for the kinase inhibitor, imatinib. On the other hand, the expression pattern of PDGFRβ was associated with good clinical outcome in NB similar to KIT. PDGFRβ has been considered to have oncogenic potential compared to PDGFRα [14].

FLT3 expression was associated with a good clinical outcome of NB in our study. Our results may provide the evidence that neuroectodermal and hematopoietic cells share common regulatory pathways, as previously reported [15]. It was reported that the RET and TRKA pathways collaborate to regulate NB differentiation [16], but RET expression was not associated with TRKA expression or any clinical parameters in present study. We could not find the alternative spliced variant form of TRKA, TRKAIII, which was reported to have the oncogenic potential [20]. We found another new isoform (deletion of exons 7–9) in 6 (25%) of 24 cell lines. Further study is needed to clarify the function of this new isoform.

In conclusion, our data suggest that the loss of expression of several RTKs may be related to disease progression and poor clinical outcome in NB.

ACKNOWLEDGMENT

We thank Junko Takita, M.D., Hirokazu Kimura, Ph.D., and Yuyan Chen, M.D. for technical assistances. Supported by a Grant-in-Aid for Cancer Research, Research on Children and Families from the Ministry of Health, Labor, and Welfare of Japan, a Grant-in-Aid for Scientific Research (C) and Exploratory Research from the Ministry of Education, Culture, Sports, Science and Technology of Japan, and a Research grant for Gunma Prefectural Hospitals.

REFERENCES

1. Robinson DR, Wu YM, Lin SF. The protein tyrosine kinase family of the human genome. Oncogene 2000;19:5548–5557.
2. Shawver LK, Slamon D, Ullrich A. Smart drugs: Tyrosine kinase inhibitors in cancer therapy. Cancer Cell 2002;1:117–123.
3. Krause DS, Van Etten RA. Tyrosine kinases as targets for cancer therapy. N Engl J Med 2005;353:172–187.
4. Vitali R, Cesi V, Nicotra MR, et al. c-Kit is preferentially expressed in MYCN-amplified neuroblastoma and its effect on cell proliferation is inhibited in vitro by STI-571. Int J Cancer 2003; 106:147–152.

5. Beppu K, Jaboine J, Merchant MS, et al. Effect of imatinib mesylate on neuroblastoma tumorigenesis and vascular endothelial growth factor expression. J Natl Cancer Inst 2004;96: 46–55.
6. Te Kronnie G, Timeus F, Rinaldi A, et al. Imatinib mesylate (STI571) interference with growth of neuroectodermal tumour cell lines does not critically involve c-Kit inhibition. Int J Mol Med 2004;14:373–382.
7. Krams M, Parwaresch R, Sipos B, et al. Expression of the c-kit receptor characterizes a subset of neuroblastomas with favorable prognosis. Oncogene 2004;23:588–595.
8. Korja M, Finne J, Salmi TT, et al. No GIST-type c-kit gain of function mutations in neuroblastic tumours. J Clin Pathol 2005;58: 762–765.
9. Uccini S, Mannarino O, McDowell HP, et al. Clinical and molecular evidence for c-kit receptor as a therapeutic target in neuroblastic tumors. Clin Cancer Res 2005;11:380–389.
10. Hirota S, Isozaki K, Moriyama Y, et al. Gain-of-function mutations of c-kit in human gastrointestinal stromal tumors. Science 1998; 279:577–580.
11. Shimada A, Taki T, Tabuchi K, et al. KIT mutations, and not FLT3 internal tandem duplication, are strongly associated with a poor prognosis in pediatric acute myeloid leukemia with t(8;21): A study of the Japanese Childhood AML Cooperative Study Group. Blood 2006;107:1806–1809.
12. Matsui T, Sano K, Tsukamoto T, et al. Human neuroblastoma cells express alpha and beta platelet-derived growth factor receptors coupling with neurotrophic and chemotactic signaling. J Clin Invest 1993;92:1153–1160.
13. Corless CL, Schroeder A, Griffith D, et al. PDGFRA mutations in gastrointestinal stromal tumors: Frequency, spectrum and in vitro sensitivity to imatinib. J Clin Oncol 2005;23:5357–5364.
14. Gilbertson RJ, Clifford SC. PDGFRB is overexpressed in metastatic medulloblastoma. Nat Genet 2003;35:197–198.
15. Timeus F, Ricotti E, Crescenzio N, et al. Flt-3 and its ligand are expressed in neural crest-derived tumors and promote survival and proliferation of their cell lines. Lab Invest 2001;81:1025–1037.
16. Peterson S, Bogenmann E The RET and TRKA pathways collaborate to regulate neuroblastoma differentiation. Oncogene 2004;23:213–225.
17. Frohling S, Scholl C, Gilliland DG, et al. Genetics of myeloid malignancies: Pathogenetic and clinical implications. J Clin Oncol 2005;23:6285–6295.
18. Neff F, Noelker C, Eggert K, et al. Signaling pathways mediate the neuroprotective effects of GDNF. Ann NY Acad Sci 2002;973:70–74.
19. Mulligan LM, Kwok JB, Healey CS, et al. Germ-line mutations of the RET proto-oncogene in multiple endocrine neoplasia type 2A. Nature 1993;363:458–460.
20. Tacconelli A, Farina AR, Cappabianca L, et al. TrkA alternative splicing: A regulated tumor-promoting switch in human neuroblastoma. Cancer Cell 2004;6:347–360.
21. Kaneko M, Tsuchida Y, Mugishima H, et al. Intensified chemotherapy increases the survival rates in patients with stage 4 neuroblastoma with MYCN amplification. J Pediatr Hematol Oncol 2002;24:613–621.
22. Hiwatari M, Taki T, Tsuchida M, et al. Novel missense mutations in the tyrosine kinase domain of the platelet-derived growth factor receptor alpha(PDGFRA) gene in childhood acute myeloid leukemia with t(8;21)(q22;q22) or inv(16)(p13q22). Leukemia 2005;19:476–477.
23. Taketani T, Taki T, Sugita K, et al. FLT3 mutations in the activation loop of tyrosine kinase domain are frequently found in infant ALL with MLL rearrangements and pediatric ALL with hyperdiploidy. Blood 2004;103:1085–1088.
24. Klugbauer S, Lengfelder E, Demidchik EP, et al. High prevalence of RET rearrangement in thyroid tumors of children from Belarus after the Chernobyl reactor accident. Oncogene 1995;11:2459–2467.
25. Lee DC, Chan KW, Chan SY. RET receptor tyrosine kinase isoforms in kidney function and disease. Oncogene 2002;21:5582–5592.
26. Shimada A, Shiota G, Miyata H, et al. Aberrant expression of double-stranded RNA-dependent protein kinase in hepatocytes of chronic hepatitis and differentiated hepatocellular carcinoma. Cancer Res 1998;58:4434–4438.
27. Caruana G, Cambareri AC, Ashman LK. Isoforms of c-KIT differ in activation of signalling pathways and transformation of NIH3T3 fibroblasts. Oncogene 1999;18:5573–5581.
28. Krystal GW, Hines SJ, Organ CP. Autocrine growth of small cell lung cancer mediated by coexpression of c-kit and stem cell factor. Cancer Res 1996;56:370–376.
29. Inoue M, Kyo S, Fujita M, et al. Coexpression of the c-kit receptor and the stem cell factor in gynecological tumors. Cancer Res 1994; 54:3049–3053.
30. Hines SJ, Organ C, Kornstein MJ, et al. Coexpression of the c-kit and stem cell factor genes in breast carcinomas. Cell Growth Differ 1995;6:769–779.
31. Sihto H, Sarlomo-Rikala M, Tynninen O, et al. KIT and platelet-derived growth factor receptor alpha tyrosine kinase gene mutations and KIT amplifications in human solid tumors. J Clin Oncol 2005;23:49–57.
32. Simon R, Panussis S, Maurer R, et al. KIT (C117)-positive breast cancers are infrequent and lack KIT gene mutations. Clin Cancer Res 2004;10:178–183.
33. Boldrini L, Ursino S, Gisfredi S, et al. Expression and mutational status of c-kit in small-cell lung cancer: Prognostic relevance. Clin Cancer Res 2004;10:4101–4108.
34. Ricotti E, Fagioli F, Garelli E, et al. c-kit is expressed in soft tissue sarcoma of neuroectodermic origin and its ligand prevents apoptosis of neoplastic cells. Blood 1998;91:2397–2405.
35. Crosier PS, Ricciardi ST, Hall LR, et al. Expression of isoforms of the human receptor tyrosine kinase c-kit in leukemic cell lines and acute myeloid leukemia. Blood 1993;82:1151–1158.
36. Sakuma Y, Sakurai S, Oguni S, et al. Alterations of the c-kit gene in testicular germ cell tumors. Cancer Sci 2003;94:486–491.
37. Montone KT, van Belle P, Elenitsas R, et al. Proto-oncogene c-kit expression in malignant melanoma: Protein loss with tumor progression. Mod Pathol 1997;10:939–944.
38. Natali PG, Berlingieri MT, Nicotra MR, et al. Transformation of thyroid epithelium is associated with loss of c-kit receptor. Cancer Res 1995;55:1787–1791.
39. Tonary AM, Macdonald EA, Faught W, et al. Lack of expression of c-KIT in ovarian cancers is associated with poor prognosis. Int J Cancer 2000;89:242–250.
40. Pietras K, Sjoblom T, Rubin K, et al. PDGF receptors as cancer drug targets. Cancer Cell 2003;3:439–443.
41. Ostman A. PDGF receptors-mediators of autocrine tumor growth and regulators of tumor vasculature and stroma. Cytokine Growth Factor Rev 2004;15:275–286.
42. Carvalho I, Milanezi F, Martins A, et al. Overexpression of platelet-derived growth factor receptor alpha in breast cancer is associated with tumour progression. Breast Cancer Res 2005;7:R788–R795.

ELSEVIER

Cancer Genetics and Cytogenetics 186 (2008) 115–119

CANCER GENETICS AND CYTOGENETICS

Short communication

MNX1–ETV6 fusion gene in an acute megakaryoblastic leukemia and expression of the *MNX1* gene in leukemia and normal B cell lines

Takeshi Taketani[a,b], Tomohiko Taki[c], Masahiro Sako[d], Takefumi Ishii[d], Seiji Yamaguchi[a], Yasuhide Hayashi[e,*]

[a]*Department of Pediatrics, Shimane University Faculty of Medicine, Izumo, Shimane, Japan*
[b]*Division of Blood Transfusion, Shimane University Hospital, Matsue, Shimane, Japan*
[c]*Department of Molecular Laboratory Medicine, Kyoto Prefectural University of Medicine Graduate School of Medical Science, Kyoto, Japan*
[d]*Department of Pediatric Hematology/Oncology, Osaka City General Hospital, Osaka, Japan*
[e]*Department of Hematology/Oncology, Gunma Children's Medical Center, 779 Shimohakoda, Hokkitsu, Shibukawa, Gunma 377-8577, Japan*

Received 5 March 2008; received in revised form 11 June 2008; accepted 27 June 2008

Abstract Patients with infant acute myeloid leukemia (AML) who carry a t(7;12)(q36;p13) translocation have been reported to have a poor clinical outcome. *MNX1–ETV6* fusion transcripts (previously *HLXB9–ETV6*) were rarely detected in AML patients having t(7;12)(q36;p13). A 23-month-old girl with acute megakaryoblastic leukemia (AMKL) exhibited chromosome abnormalities, including add(7)(q22), and del(12)(p12p13). Southern blot analysis of bone marrow cells showed an *ETV6* gene rearrangement. Reverse transcriptase-polymerase chain reaction (RT-PCR) followed by sequence analysis revealed the presence of an *MNX1–ETV6* fusion gene. The patient responded well to chemotherapy, achieved complete remission, and at writing had been in complete remission for 60 months. The *MNX1* expression by RT-PCR was significantly more frequent in Epstein–Barr virus–transformed B-cell lines derived from normal adult lymphocytes than in leukemic cell lines. This represents a novel case of an AMKL patient with *MNX1–ETV6* fusion transcripts who had a good prognosis.

1. Introduction

Many recurrent chromosomal translocations are involved in acute myeloid leukemia (AML) [1]. AML with 12p13 translocations have been reported to involve the ETS variant gene 6 (*TEL* oncogene) (*ETV6*) [2]. In cases of AML carrying 12p13 abnormalities, a recurrent translocation t(7;12)(q36;p13) is found in 20%–30% of infant cases [3–5]. Fluorescence in situ hybridization assay is needed to evaluate this translocation, because it is difficult to detect by conventional karyotyping [3–5]. AML patients with this translocation are characterized by age under 20 months at diagnosis, thrombocytosis, high percentage of CD34-positive cells, presence of additional chromosomal abnormalities, including trisomy 19 or trisomy 8 (or both), and a poor prognosis [3–5]. An *MNX1–ETV6* fusion gene (previously *HLXB9–ETV6*) was identified in two pediatric AML patients having t(7;12)(q36;p13) [6]; however, heterogeneity of the 7q36 and 12p13 translocations was reported [5,7,8]. Thus, *MNX1–ETV6* fusion gene in AML patients having t(7;12) is infrequently reported [7,8].

We describe the case of a 23-month-old AML patient with add(7)(q22), del(12)(p12p13), and *MNX1–ETV6* fusion transcript; the child has remained alive for 5 years. We also report the expression of the *MNX1* gene in several leukemic and normal Epstein–Barr virus-transformed cell lines.

2. Case report

A 23-month-old girl was admitted to Osaka City General Hospital because of appetite loss and pallor. Blood examination showed a white blood cell count of 10,520/μL with 55.5% blasts, a hemoglobin level of 7.0 g/dL, and a platelet count of 164,000/μL. She had a mediastinal mass, but no hepatosplenomegaly. Bone marrow examination revealed a nuclear cell count of 30,000/μL with 71.2% blasts. The

* Corresponding author. Tel.: +81-279-52-3551, ext. 2200; fax: +81-279-52-2045.
E-mail address: hayashiy-tky@umin.ac.jp (Y. Hayashi).

0165-4608/08/$ – see front matter
doi:10.1016/j.cancergencyto.2008.06.009

blasts were negative for myeloperoxidase staining and platelet peroxidase staining electron-microscopically. Flow cytometric analysis showed that the blasts expressed CD41, CD36, CD13, CD33, CD15, and CD7 antigens, suggesting megakaryoblastic origin. Conventional G-banding chromosomal analysis revealed a karyotype of 46,XX,add (7)(q22),del(12)(p12p13) in all 20 bone marrow cells examined (Fig. 1).

The patient was diagnosed as having AMKL (M7 subtype, based on the French–American–British classification), and was treated on the Japanese Childhood AML Cooperative Study Group Protocol, AML99 [9]. She obtained complete remission with induction chemotherapy (cytarabine, etoposide, and mitoxantrone). Thereafter, she was treated with five additional courses of intensive chemotherapy (high-dose cytarabine, etoposide, idarubicin, and mitoxantrone). As of writing, she had been in complete remission for 60 months after diagnosis.

3. Materials and methods

3.1. Southern blot analysis

High molecular weight DNA was extracted from bone marrow cells of the patient by proteinase K digestion and phenol–chloroform extraction [10]. Ten micrograms of DNA was digested with *Eco*RI, subjected to electrophoresis on 0.7% agarose gels, and transferred to nylon membrane, and hybridized to cDNA probes ^{32}P-labeled by the random hexamer method [10]. The probes used were a 516-bp *MNX1* cDNA fragment (nucleotide nt598 to nt1114; GenBank accession no. NM_005515; previously *HLXB9*).

3.2. Expression of WT1 mRNA and mutation of FLT3

WT1 mRNA was examined for detection of minimal residual disease as previously reported [11]. Internal tandem duplication and mutation of *FLT3* were examined as previously reported [10].

3.3. Reverse transcriptase–polymerase chain reaction and nucleotide sequencing

MNX1–ETV6 chimeric mRNA was detected by reverse transcriptase–polymerase chain reaction (RT-PCR) as described previously [12]. Total RNA was extracted from the leukemic cells of the patient using the acid guanidine thiocyanate–phenol chloroform method [12]. Total RNA (4 μg) was reverse-transcribed to cDNA, using a cDNA synthesis kit (GE Healthcare Bio-Science, Piscataway, NJ) [12]. PCR was performed with AmpliTaq Gold DNA polymerase (Applied Biosystems, Foster City, CA; Tokyo, Japan), using the reagents recommended by the manufacturer. The primers used and PCR conditions were as described previously [6]. The PCR products were subcloned into pCR2.1 vector (Invitrogen, Carlsbad, CA) and sequenced by the fluorometric method using the BigDye Terminator cycle sequencing kit (Applied Biosystems).

3.4. Expression of the MNX1 gene by RT-PCR in leukemic cell lines

To analyze the expression pattern of the *MNX1* gene in leukemic cell lines, RT-PCR was performed. Fifty-nine cell lines were examined, as follows [12]; 10 B-precursor ALL cell lines (LC4-1, NALM-6, NALM-24, NALM-26, UTP-2, RS4;11, SCMC-L10, KOCL-33, KOCL-45, KOCL-69), 9

Fig. 1. G-banding karyotype of the leukemic cells in a pediatric patient with acute megakaryoblastic leukemia: 46,XX,add(7)(q22),del(12)(p12p13).

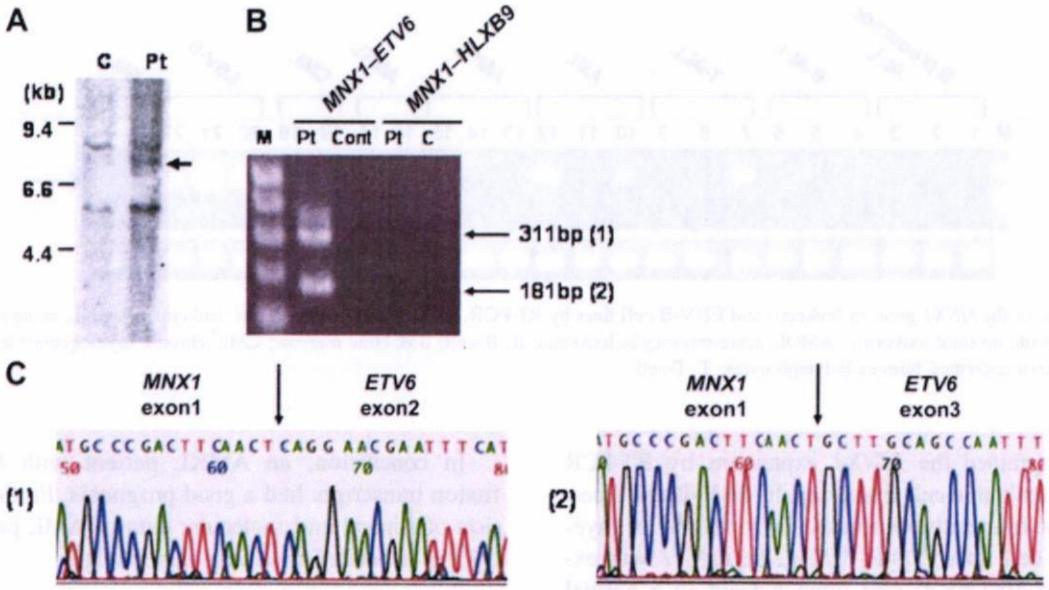

Fig. 2. Detection of the *MNX1–ETV6* fusion gene (previously *HLXB9–ETV6*). (A) Rearrangement of the *MNX1* gene by Southern blotting with *Eco*RI digestion. The arrow indicates a rearranged band of the *MNX1* gene; C, control; Pt, patient. (B) The *MNX1–ETV6* fusion transcript identified by reverse transcriptase–polymerase chain reaction (RT-PCR). Lanes 2 and 3, *MNX1–ETV6* fusion transcript; lanes 4 and 5, *ETV6–MNX1* fusion transcript. C, control; M, size marker; Pt, patient; (C) Nucleotide and amino acid sequencing of two *MNX1–ETV6* fusion transcripts.

B-ALL cell lines (BALM-1, BALM-13, BALM-14, BJAB, DAUDI, RAJI, RAMOS, BAL-KH, NAMALLA), 9 T-ALL cell lines (RPMI-8402, MOLT-14, THP-6, PEER, H-SB2, HPB-ALL, L-SAK, L-SMY, KCMC-T), 8 AML cell lines (YNH-1, ML-1, KASUMI-3, KG-1, inv-3, SN-1, NB4, HEL), 6 acute monocytic leukemia cell lines (THP-1, IMS/M1, CTS, P31/FUJ, MOLM-13, KOCL-48), 5 chronic myelogenous leukemia cell lines (MOLM-1, MOLM-7, TS9;22, SS9;22, K-562), 2 acute megakaryoblastic leukemia cell lines (CMS, CMY), and 10 Epstein-Barr virus transformed B lymphocyte (EBV-B) cell lines derived from normal adult peripheral lymphocytes. Five normal BM samples were also examined. RT-PCR mixtures and conditions were the same as described [10]. The primers used for RT-PCR were HLXB9-658F (5′-GGCATGATCCTGCCTAAGAT-3′) (sense primer) and HLXB9-1092R (TGCT GTAGGGGAAATGGTCGTCG) (antisense primer) [6].

4. Results and discussion

The karyotype of the patient's leukemic cells was 46,XX,add(7)(q22),del(12)(p12p13), suggesting that both *ETV6* and *MNX1* were involved in this chromosomal abnormality. With informed consent from the patient's parents, DNA and total RNA were extracted from bone marrow cells of the patient. Southern blot analysis of DNA from leukemic cells of the patient using the *MNX1* probe showed a rearranged band (Fig. 2A). We performed RT-PCR for *MNX1–ETV6* chimeric mRNA and obtained two RT-PCR products, of 311 bp and 181 bp (Fig. 2B). Sequence analysis of these PCR products showed that one product was an in-frame fusion transcript of exon 1 of *MNX1* to exon 3 of *ETV6*, and the other was an out-of-frame fusion transcript of exon 1 of *MNX1* to exon 2 of *ETV6* (Fig. 2C). These transcripts were the same as previously reported [6]. The reciprocal *ETV6–MNX1* transcript was not detected (Fig. 2B).

The *WT1* mRNA level was 3,400 copies/μg RNA at diagnosis, but decreased to <50 copies/μg RNA after remission. Neither internal tandem duplication nor mutation of *FLT3* were found in this patient, suggesting that the prognosis is not poor [1].

Table 1
Expression of the *MNX1* gene in leukemia and EBV-B cell lines by reverse transcriptase–polymerase chain reaction

Cell line	Cells examined, no.	Cells expressing *MNX1*, no. (%)
ALL	28	5 (17.9)
B precursor	10	0 (0)
B	9	2 (22.2)
T	9	3 (33.3)
AML	16	3 (18.8)
AML	8	1 (12.5)
AMoL	6	2 (33.3)
AMKL	2	0 (0)
CML	5	1 (20)
EBV-B	10	7 (70)
normal BM	5	0 (0)

Abbreviations: ALL, acute lymphoblastic leukemia; AMKL, acute megakaryoblastic leukemia; AML, acute myeloid leukemia; AMoL, acute monocytic leukemia; B, B-cell; BM, bone marrow; CML, chronic myelogenous leukemia; EBV-B, Epstein–Barr virus-transformed human B lymphocytes; T, T-cell.

Fig. 3. Expression of the *MNX1* gene in leukemia and EBV-B cell lines by RT-PCR. ALL, acute lymphoblastic leukemia; AMKL, acute megakaryoblastic leukemia; AML, acute myeloid leukemia; AMOL, acute monocytic leukemia; B, B-cell; BM, bone marrow; CML, chronic myelogenous leukemia; EBV-B, Epstein–Barr virus-transformed human B lymphocytes; T, T-cell.

We next examined the *MNX1* expression by RT-PCR analysis in 49 leukemic cell lines, and 10 EBV-B cell lines. *MNX1* was not frequently expressed in lymphoid or myeloid leukemic cell lines (Table 1; Fig. 3). *MNX1* was expressed in 7 of 10 EBV-B cell lines, but not in 5 normal BM cells. The *MNX1* expression was significantly more frequent in EBV-B cell lines than in leukemic cell lines ($P = 0.0015$) or in normal BM cells ($P = 0.0256$). The *MNX1* was frequently expressed in CD34-positive cells purified from normal BM cells, acute leukemia cells, and AML cells having t(7;12)(q36;p13) [5,13,14]. It is unknown whether the incidence of *MNX1* expression differs among leukemia cell lines. Mature B-lineage cells are likely to frequently express *MNX1* transcripts, and the transcripts were more prevalent in several human B lineage cell line and tonsil B cells [15]. The present findings are compatible with previous reports. *MNX1* may be associated with differentiation of B cells.

MNX1–ETV6 fusion transcript has so far been detected in only four out of the many AML patients who carry the t(7;12) anomaly [5,6]. Difficulty of detection of this fusion transcript is due to breakpoint heterogeneity of the 7q36 and 12p13 in this translocation [7,8]. Clinical features of AML patients having t(7;12) did not differ between the presence and absence of *MNX1–ETV6* fusion transcripts [5]. Notably, clinical characteristics of the present patient were different from those of AML patients having t(7;12) previously reported. Our patient was diagnosed as having AMKL, although most AML patients having t(7;12) were identified as poorly differentiated FAB subtypes [5]. Only one patient was reported to be diagnosed with AMKL; however, *MNX1–ETV6* fusion transcript was not examined in that case [4]. An additional cytogenetic abnormality is trisomy 19 [3–5]. Chromosomal analysis of the present patient showed absence of additional chromosomal abnormalities, suggesting long-term disease-free survival with chemotherapy alone. All AML patients, except one who had both t(7;12) and trisomy 19, died [3–6]. These findings suggest that t(7;12) is associated only with leukemogenesis, and that other factors including trisomy 19 and *FLT3* mutations, may affect the prognosis of AML patients having t(7;12).

In conclusion, an AMKL patient with *MNX1–ETV6* fusion transcripts had a good prognosis. Further accumulation of clinical and molecular data of AML patients having t(7;12) is needed to clarify this result.

Acknowledgments

We express our appreciation to Mrs. Shoko Sohma and Hisae Soga for their excellent technical assistance. We thank Dr. Takeyuki Sato, Department of Pediatrics, Chiba University School of Medicine, Japan, for providing AMKL (CMS, CMY) cell lines; Dr. Kanji Sugita, Department of Pediatrics, Yamanashi University School of Medicine, Japan, for providing ALL (KOCL-33, -45, -69) cell lines and AMoL (KOCL-48) cell lines; and Dr. Yoshinobu Matsuo, Hayashibara Biochemical Laboratories, Inc., Fujisaki Cell Center, Japan, for providing varieties of ALL cell lines. This work was supported by a Grant-in-Aid for Cancer Research, Research on Children and Families from the Ministry of Health, Labor, and Welfare of Japan, a Grant-in-Aid for Scientific Research (C), and Exploratory Research from the Ministry of Education, Culture, Sports, Science, and Technology of Japan.

References

[1] Hayashi Y. The molecular genetics of recurring chromosome abnormalities in acute myeloid leukemia. Semin Hematol 2000;37:368–80.

[2] Bohlander SK. *ETV6*: a versatile player in leukemogenesis. Semin Cancer Biol 2005;15:162–74.

[3] Tosi S, Harbott J, Teigler-Schlegel A, Haas OA, Pirc-Danoewinata H, Harrison CJ, Biondi A, Cazzaniga G, Kempski H, Scherer SW, Kearney L. t(7;12)(q36;p13), a new recurrent translocation involving *ETV6* in infant leukemia. Genes Chromosomes Cancer 2000;29:325–32.

[4] Slater RM, von Drunen E, Kroes WG, Weghuis DO, van den Berg E, Smit EM, van der Does-van den Berg A, van Wering E, Hählen K, Carroll AJ, Raimondi SC, Beverloo HB. t(7;12)(q36;p13) and t(7;12)(q32;p13): translocations involving *ETV6* in children 18 months of age or younger with myeloid disorders. Leukemia 2001;15:915–20.

[5] von Bergh AR, van Drunen E, van Wering ER, van Zutven LJ, Hainmann I, Lönnerholm G, Meijerink JP, Pieters R, Beverloo HB.

High incidence of t(7;12)(q36;p13) in infant AML but not in infant ALL, with a dismal outcome and ectopic expression of *HLXB9*. Genes Chromosomes Cancer 2006;45:731–9.

[6] Beverloo HB, Panagopoulos I, Isaksson M, van Wering E, van Drunen E, de Klein A, Johansson B, Slater R. Fusion of the homeobox gene *HLXB9* and the *ETV6* gene in infant acute myeloid leukemias with the t(7;12)(q36;p13). Cancer Res 2001;61:5374–7.

[7] Simmons HM, Oseth L, Nguyen P, O'Leary M, Conklin KF, Hirsch B. Cytogenetic and molecular heterogeneity of 7q36/12p13 rearrangements in childhood AML. Leukemia 2002;16:2408–16.

[8] Tosi S, Hughes J, Scherer SW, Nakabayashi K, Harbott J, Haas OA, Cazzaniga G, Biondi A, Kempski H, Kearney L. Heterogeneity of the 7q36 breakpoints in the t(7;12) involving *ETV6* in infant leukemia. Genes Chromosomes Cancer 2003;38:191–200.

[9] Shimada A, Taki T, Tabuchi K, Tawa A, Horibe K, Tsuchida M, Hanada R, Tsukimoto I, Hayashi Y. *KIT* mutations, and not *FLT3* internal tandem duplication, are strongly associated with a poor prognosis in pediatric acute myeloid leukemia with t(8;21): a study of the Japanese Childhood AML Cooperative Study Group. Blood 2006;107:1806–9.

[10] Taketani T, Taki T, Sugita K, Furuichi Y, Ishii E, Hanada R, Tsuchida M, Sugita K, Ida K, Hayashi Y. *FLT3* mutations in the activation loop of tyrosine kinase domain are frequently found in infant ALL with *MLL* rearrangements and pediatric ALL with hyperdiploidy. Blood 2004;103:1085–8.

[11] Inoue K, Ogawa H, Yamagami T, Soma T, Tani Y, Tatekawa T, Oji Y, Tamaki H, Kyo T, Dohy H, Hiraoka A, Masaoka T, Kishimoto T, Sugiyama H. Long-term follow-up of minimal residual disease in leukemia patients by monitoring *WT1* (Wilms tumor gene) expression levels. Blood 1996;88:2267–78.

[12] Taketani T, Taki T, Shibuya N, Kikuchi A, Hanada R, Hayashi Y. Novel *NUP98–HOXC11* fusion gene resulted from a chromosomal break within exon 1 of *HOXC11* in acute myeloid leukemia with t(11;12)(p15;q13). Cancer Res 2002;62:4571–4.

[13] Deguchi Y, Kehrl JH. Selective expression of two homeobox genes in CD34-positive cells from human bone marrow. Blood 1991;78:323–8.

[14] Deguchi Y, Yamanaka Y, Theodossiou C, Najfeld V, Kehrl JH. High expression of two diverged homeobox genes, HB24 and HB9, in acute leukemias: molecular markers of hematopoietic cell immaturity. Leukemia 1993;7:446–51.

[15] Harrison KA, Druey KM, Deguchi Y, Tuscano JM, Kehrl JH. A novel human homeobox gene distantly related to proboscipedia is expressed in lymphoid and pancreatic tissues. J Biol Chem 1994;269:19968–75.

Whole-genome profiling of chromosomal aberrations in hepatoblastoma using high-density single-nucleotide polymorphism genotyping microarrays

Makoto Suzuki,[1,6] Motohiro Kato,[2] Chen Yuyan,[2] Junko Takita,[3] Masashi Sanada,[4] Yasuhito Nannya,[4] Go Yamamoto,[4] Atsushi Takahashi,[1] Hitoshi Ikeda,[6] Hiroyuki Kuwano,[1] Seishi Ogawa[5,8] and Yasuhide Hayashi[7,8]

[1]Department of General Surgical Science, Graduate School of Medicine, Gunma University Graduate School, 3-39-15 Showa, Maebashi, Gunma 371-8511; [2]Department of Pediatrics, [3]Department of Cell Therapy and Transplantation Medicine, [4]Department of Hematology and Oncology, and [5]The 21st century COE program, Graduate School of Medicine, University of Tokyo, 7-3-1 Hongo, Bunkyo-ku, Tokyo 113-8655; [6]Department of Pediatric Surgery, Koshigaya Hospital, Dokkyo Medical School, 2-1-50 Minami-Koshigaya, Koshigaya, Saitama 343-8555; [7]Department of Hematology and Oncology, Gunma Children's Medical Center, 779 Shimohakoda, Hokkitsu, Shibukawa, Gunma 377-8577, Japan

(Received July 31, 2007/Revised November 14, 2007/Accepted November 17, 2007/Online publication January 2, 2008)

To identify the genomic profile and elucidate the pathogenesis of hepatoblastoma (HBL), the most common pediatric hepatic tumor, we performed high-density genome-wide single-nucleotide polymorphism (SNP) microarray analyses of 17 HBL samples. The copy number analyzer for GeneChip® (CNAG) and allele-specific copy number analysis using anonymous references (AsCNAR) algorithms enabled simple but sensitive inference of allelic composition without using paired normal DNA. Chromosomal aberrations were observed in 15 cases (88%). Gains in chromosomes 1q, 2 (or 2q), 8, 17q, and 20 and losses in chromosomes 4q and 11q were frequently identified. High-grade amplifications were detected at 7q34, 14q11.2, and 11q22.2. Several types of deletions, except homozygous deletion, were identified. Most importantly, copy-neutral loss of heterozygosity (uniparental disomy [UPD]) at 11p15 was detected in four of the 17 HBL samples. Insulin-like growth factor II (*IGF2*) and *H19* genes were located within this region. The methylated status of this region indicated the paternal origin of the UPD. The expression patterns of *IGF2* and *H19* were opposite between genes with and without the UPD. This difference in the expression patterns might influence the clinical features of HBL. (*Cancer Sci* 2008; 99: 564–570)

Hepatoblastoma (HBL) is the most common pediatric hepatic tumor predominantly observed in infants and children aged less than 3 years.[1–3] The dramatic increase in the survival of patients that has been observed during the last three decades is mainly due to advances in the use of chemotherapy and surgical techniques.[1–3] Currently, approximately 75% of children with HBL can be cured completely, although a large tumor, a multifocal tumor, and metastatic spread are all associated with a fatal outcome.[3] The etiology of HBL remains unknown. Most HBL are sporadic; however, an association with prematurity or low birth weight,[4] and genetic disorders such as familial adenomatous polyposis (FAP),[5] or Beckwith–Wiedemann syndrome (BWS) has been documented.[6] These findings imply that an alteration at 11p15, which is the critical region in BWS and critical to the wingless signaling pathway involving the adenomatosis polyposis coli (*APC*) gene that is constitutionally mutated in FAP patients,[7,8] could also play a role in the genesis of sporadic HBL. Indeed, the loss of heterozygosity (LOH) at 11p15 and mutations in the *APC* and β-catenin genes have also observed in some sporadic HBL.[9,10]

LOH and deletion of tumor suppressor genes are observed frequently in malignant cells and can be associated with the deregulation of cell fate and apoptosis.[11] Similarly, amplification of the chromosomal regions can increase the expression of oncogenes during tumor progression. Conventional cytogenetic analyses of chromosomal aberrations in HBL performed using standard karyotyping,[12–16] fluorescence *in situ* hybridization (FISH),[17–20] and comparative genomic hybridization (CGH),[21,22] have been reported. Although these analyses have identified several chromosomal aberrations in HBL, predominantly the gains in chromosomes 1q, 2, 8q, 17q, and 20 and the loss in chromosome 4q, the tumor-associated genes of HBL involved in these genomic copy number (CN) alterations are yet to be identified.

In recent years, a high-resolution genomic approach has been used for the systematic screening of chromosomal CN alterations. The availability of microarray-based high-density single-nucleotide polymorphism (SNP) analysis allows a reproducible and rapid determination of genome-wide alterations.[23–25] The Affymetrix® GeneChip® platform, originally developed for large-scale SNP typing, has a unique feature compared with array-based CGH: it enables the genome-wide detection of LOH in addition to extremely high-resolution CN analysis of cancer genomes by using large numbers of SNP-specific probes. The density, distribution, and allele specificity of SNP render them an excellent candidate for the high-resolution analyses of LOH and CN alterations in cancer genomes.[26,27] Conventionally, LOH analyses require the comparison of the genotypes of the tumor and its normal germline counterpart. However, for the analysis of cell line, xenograft, leukemia, and archival samples, paired normal DNA is often unavailable. In the absence of a paired normal DNA sample, LOH is inferred only based on the lower-than-expected frequencies of heterozygous SNP calls in the tumor samples. However, the low tumor content within the samples greatly hampers the sensitive detection of LOH due to increased heterozygous SNP calls. To overcome these difficulties with the current algorithms, we have recently developed novel algorithms (copy number analyzer for GeneChip® [CNAG] and allele-specific copy number analysis using anonymous references [AsCNAR]) to analyze the allelic composition of cancer genomes based on the microarray data obtained from the GeneChip® platform.[27,28] These algorithms calculate the allele-specific CN independent of the availability of a paired control DNA, enabling the sensitive detection of both LOH and CN alterations in a wide spectrum of primary tumor specimens. The performance of the new algorithm was demonstrated by detecting the neutral CN LOH or uniparental disomy (UPD) in a large number of acute leukemia samples.[28]

[8]To whom correspondence should be addressed.
E-mail: hayashiy-tky@umin.ac.jp; sogawa-tky@umin.ac.jp

doi: 10.1111/j.1349-7006.2007.00710.x

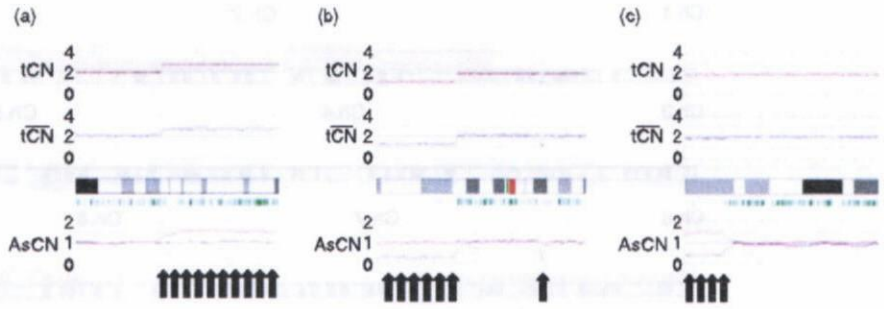

Fig. 1. Representative results of the allele-specific copy number analysis using anonymous references (AsCNAR) program with regard to copy number (CN) alterations detected in our series at particular loci, such as (a) gain (b) chromosomal loss, and (c) uniparental disomy (UPD), which have not been detected using conventional algorithms. The red dots indicate the raw CN plot for each single-nucleotide polymorphism (SNP), and the blue lines indicate the local mean CN of five SNP. The vertical green bar indicates the heterozygous SNP calls.

In the present study, to identify the novel genomic alterations in sporadic HBL cases, we performed high-resolution analyses of genome-wide CN alterations such as gains, losses, allelic imbalances, and amplifications of small chromosomal regions. Due to the high resolution of the SNP arrays and the new algorithm AsCNAR, we could systematically identify several amplifications, deletions, and allelic imbalances, including the UPD.

Materials and Methods

Patients and samples. We obtained 17 primary HBL samples at the time of diagnosis from five patients treated at the Gunma Children's Medical Center and 12 patients treated at different institutes in Japan, including Saitama Children's Medical Center. No patient had received chemo- and/or radiotherapy before the biopsy of the primary tumors. After obtaining informed consent from the parents and approval for the study from the institutional review board of each institute, all the HBL samples were subjected to genomic DNA extraction using the QIAamp DNA Mini Kit (Qiagen, Chatsworth, CA, USA) according to the manufacturer's instructions. Total RNA was extracted from the frozen stocked tumors using the Isogen reagent (Nippon Gene, Osaka, Japan), according to the manufacturer's instructions. The total RNA was reverse transcribed to synthesize cDNA using the Ready-To-Go T-Primed First-Strand Kit (GE Healthcare Bio-Sciences, Piscataway, NJ, USA).

SNP array analysis. The array experiments were performed according to the standard protocol of Affymetrix® GeneChip® Mapping 50K *Xba*I Array (Affymetrix, Inc., Santa Clara, CA, USA). In brief, the total genomic DNA (250 ng from each sample) was first digested with a restriction enzyme (*Xba*I). The digested DNA was then ligated to an appropriate adapter that recognized the four cohesive base pair (bp) overhangs, and polymerase chain reaction (PCR) amplification was performed using a single primer that recognized the adapter sequence. After fragmentation with DNase I, the PCR products were labeled with a biotinylated nucleotide analog using terminal deoxynucleotidyl transferase, and the labeled products were hybridized to the GeneChip® Human Mapping 50K Array for 17 h. Subsequently, the arrays were washed, stained, and scanned.

The genotype calls and the intensity of the SNP probes were determined using GeneChip Operation software (GCOS; Affymetrix, Inc.). The SNP CN and chromosomal regions with gains or losses were individually evaluated using the CNAG[27] and AsCNAR algorithms,[28] which enabled an accurate determination of allele-specific CN as well as the sensitive detection of LOH even in the presence of normal cell contamination of up to 70–80% without requiring constitutive DNA (Fig. 1; http://www.genome.umin.jp).

Validation of CN alterations using the interphase FISH. We performed FISH to validate the CN status obtained using the SNP array analysis. FISH probes were prepared using the BAC clones RP11-185M22, RP11-80P10, and RP11-86M15. Each BAC DNA was purified, and 100 ng of the clone was labeled with digoxigenin-dUTP using random primers; these labeled clones were used as probes for FISH analysis by following the established protocols.[29,30]

Quantitative real-time PCR and reverse transcription (RT)-PCR. Real-time quantitative PCR (RQ-PCR) and real-time quantitative RT-PCR (RQ-RT-PCR) analyses were carried out to quantify the relative CN of several amplifications in the HBL samples and the expression levels of the defender against cell death 1 (*DAD1*), EPH receptor B6 (*EphB6*), *ErbB4*, insulin-like growth factor II (*IGF2*), and *H19* genes using a Power SYBR Green PCR Master Mix (Applied Biosystems, Foster City, CA, USA) with an ABI prism 7700 real-time PCR detection system (Applied Biosystems). The primer pairs were designed using PrimerExpress software (Applied Biosystems) and synthesized by Invitrogen (Carlsbad, CA, USA).The primer sets used for the RQ-PCR experiments are listed in Table 1. Data were captured using Sequence Detection

Table 1. Primers used for polymerase chain reaction (PCR) analyses

Gene	Primer forward	Primer reverse
(Genomic RQ-PCR)		
EphB6	GGACTGCAACTGAACGTCAA	TCTGGAAAGGAAGCAAAGGA
DAD1	GTTATGTCGGCGTCGGTAGT	GTCCCCACGAGGAGACAGTA
(RQ-RT-PCR)		
ERBB4	AACAGCAGTACCGAGCCTTG	CCAGAGGCAGGTAACGAAAC
DAD1	CGAGCCTTTGCTGATTTTCT	TCCAATAAGCTGCCATCTCC
IGF2	CTCTCCGTGCTGTTCTCTCC	TATCGGGAAATGAGGTCAGC
H19	GAAGGAGGTTTAGGGGATCG	TTGCTCTTTCTGCCTGGAAC
(Bisulfite PCR/RQ-PCR)		
H19DMR (Methylated)	GGTACGGTTTTTTTAGGTTTATGTC	ACCCCTACAACCTCCTTACTACG
H19DMR (Unmethylated)	TATGGTTTTTTTAGGTTTATGTTGG	ACCCCTACAACCTCCTTACTACAC

Primers and probes were designed using Primer Express software and MethPrimer software. RQ-PCR, real-time quantitative PCR; RQ-RT-PCR, real-time quantitative reverse transcription-PCR.

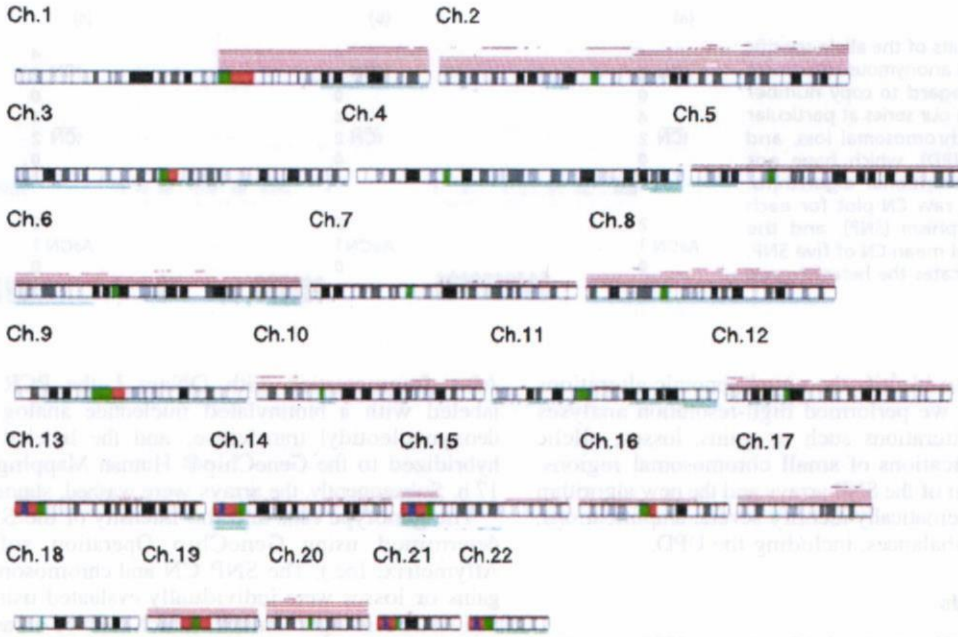

Fig. 2. Overview of the DNA copy number (CN) gains and losses detected in 17 hepatoblastoma (HBL) samples. A gain is indicated by the red bar above the chromosome ideogram, and a loss is indicated by the green bar under the chromosome ideogram. Each horizontal line represents an aberration detected in a single tumor.

software (version 1.7a; Applied Biosystems). For each primer pair, a standard curve was generated from five-fold serial dilution from approximately 50–80 pg of control DNA from a healthy individual. The amounts of genomic DNA and cDNA used in each test and the reference marker for all HBL samples were calculated using the appropriate standard curve. Normalization was performed using the β-actin gene as the internal control.

Sodium bisulfite modification and methylation-specific PCR. The genomic DNA from the tumor samples was treated with sodium bisulfite as described previously.[31] Briefly, 1 μg of DNA was denatured with sodium hydroxide and modified with sodium bisulfite. The modified DNA was then purified with the Wizard® DNA Clean-Up System (Promega, Madison, WI, USA), precipitated with ethanol, resuspended in Tris-EDTA (TE) buffer (pH 8.0), and either used immediately or stored at –20°C until use. The bisulfite-modified DNA was amplified with primer pairs for the methylated and unmethylated complete sequences upstream of the *H19* promoter CpG islands in the HBL samples with UPD in 11p15. The primer pairs were designed using MethPrimer software,[32] and synthesized by Invitrogen. The primers for methylation-specific DNA and unmethylation-specific primers are listed in Table 1. Normal lymphocyte DNA was used as the control. PCR was carried out in a 25 μL reaction volume using Ex Taq Hot Start Version (TaKaRa Bio Inc., Kyoto, Japan). The PCR conditions were as follows: 1 cycle at 95°C for 10 min; followed by 35 cycles of 94°C for 30 s, 60°C for 30 s, 72°C for 2 min; and a final extension at 72°C for 5 min. The PCR products were separated on 3% agarose gels and visualized under UV illumination after ethidium bromide staining. To quantify the ratio of the methylation status, we also carried out the methylation-specific RQ-PCR analysis.

Results

Detection of CN alterations in HBL samples. We investigated 17 HBL samples obtained from the sporadic cases of HBL by using the Affymetrix® GeneChip® 50K *Xba*I Mapping Array. Although these specimens did not contain paired control DNA and had varying degrees of normal tissue contamination, the genomic alterations were accurately determined in most specimens by our CNAG/AsCNAR program (Fig. 1). The real CN and LOH status was inferred from the observed signal ratios of the tumor to the reference, based on the hidden Markov models implemented in the CNAG/AsCNAR program; these are summarized in Fig. 2. The CN data were validated at a number of SNP sites using FISH analysis of the cell nuclei extracted from the HBL samples (Fig. 3). The CN data obtained using the FISH analyses were consistent with those obtained using SNP mapping.

Numerical chromosomal aberrations were observed in 15 HBL samples (88%), excluding two HBL samples (HBL_22 and HBL_250). These 15 cases had variable degrees of CN gains and losses; however, the gains including the amplifications were more frequent than the losses (Table 2 and Fig. 2). Total or partial gains in chromosomes 1q and 2 were the most frequent aberrations detected in eight of the 17 patients (47%). The gain in chromosome 8 was the second most frequent aberration detected in five of the 17 samples (29%). The gains in chromosomes 17q and 20 were observed in 24% of the cases (four of 17 cases). The LOH in chromosomes 4q and 11q was observed in three (18%) and two (12%) of the 17 samples, respectively. However, these regions were usually large, and we could not determine the presence or absence of alterations in specific genes within these regions.

High-grade amplification and common deletion. High-grade amplifications are of particular interest because they may indicate the loci of oncogenes. The regions with high-grade amplification were defined as segments with at least five SNP loci with an inferred CN of >5. High-grade amplifications of 7q34 and 14q11.2 were observed in five (29%) and nine (53%) HBL samples, respectively. For the validation of the amplifications observed using the SNP array, FISH analysis and genomic RQ-PCR were performed. To determine the genes that are potentially affected at 14q11.2, several genes localized at the 14q11.2 chromosomal region with overlap or proximity to the BAC-RP11-85M16 were examined using the UCSC browser (www.genome.ucsc.edu). Genes that map to these regions include *EphB6* and *DAD1*, which are identified as the negative regulators of apoptosis. These two genes were subjected to RQ-PCR. FISH analysis with RP11-85M16 BAC clone probe showed multiple signals, confirming

doi: 10.1111/j.1349-7006.2007.00710.x

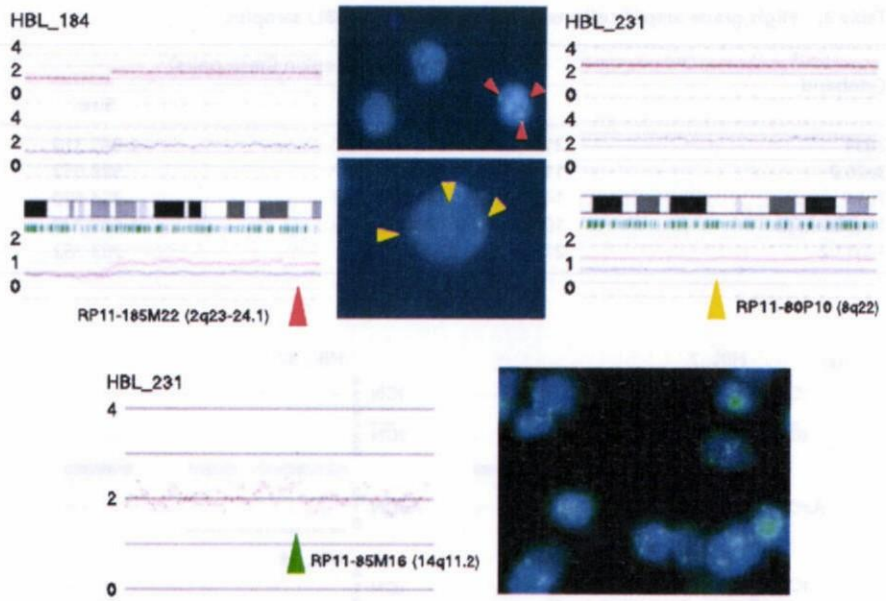

Fig. 3. Representative results of array analysis of hepatoblastoma (HBL) samples (HBL_184 and HBL_231). Fluorescent *in situ* hybridization analysis with BAC probes confirmed the detected changes. We detected three signals from chromosomes 2q and 8q. At the high-amplification region of chromosome 14q, three and more signals were detected.

Table 2. Chromosomal aberrations in 17 primary hepatoblastoma (HBL) samples

Sample	Copy number gain	Copy number loss	Uniparental disomy
HBL_4	1q, 2q34, 5p13.1, 17q23.3-qter	3p13-pter, 3q13.11, 6q14.1-qter, 11q23.1-qter	Not detected
HBL_7	1q, 2, 8, 14q11.2, 20	not detected	11p15.4-pter
HBL_8	7q34	not detected	Not detected
HBL_9	1q, 2q14.1-qter, 6p, 7, 14q11.2	6p12.1, 9p21.1	Not detected
HBL_12	8q11.23, 10q21.3, 10q26.13, 14q11.2, 22q13.31	7q35	Not detected
HBL_14	2p16.3-p22.3, 2p23.1, 2q11.2-q14.1, 2q33.1-q34, 3p21.33-p22.1, 3p24.2, 3p25.1, 3p25.2, 4q32.2-q32.3, 5p13.2, 6q14.3-q16.1, 7q, 11p15.1, 10p13-pter, 11q22.2-q22.3, 12p13.2-pter, 14q23.3-q31.1, 15q22.31-q26.2, 16p12.3, 20p11.23	1q31.1-qter, 2p12-14, 3, 4q, 5p14.1-pter, 5q32-qter, 6p12.13-pter, 6q11.1, 6q25.1-qter, 8, 9, 12p11.1-13.1, 17q24.3, 18p11.21-11.32, 18q21.1-qter, 19, 22	Not detected
HBL_22	Not detected	Not detected	Not detected
HBL_27	1q, 2q24.2-24.3, 7q34, 14q11.2	4q32.3-qter, 16p12.1	Not detected
HBL_28	3p26.1, 7q34, 14q11.2, 20	2p24.1	11p14.3-pter
HBL_34	1q, 2, 7q34, 14q11.2, 17	4q34.1-qter	Not detected
HBL_36	1q32.1-qter	1p13.3-pter, 4q21.22-qter, 5p13.1	Not detected
HBL_37	1q, 2, 5, 6, 7q34, 8, 10, 12, 14, 14q11.2, 15, 16q22.1-pter, 17, 19, 20	Not detected	11p15.2-pter, 16q22.2-qter
HBL_184	2q14.2-qter, 3p24.3, 4q33, 10p14, 11p14.3, 14q11.2	Not detected	Not detected
HBL_185	6p, 21q21.2	Not detected	Not detected
HBL_231	8, 14q11.2, 19, 20	Not detected	11p15.4-pter
HBL_246	1q, 2, 5, 6, 8, 10, 12, 13, 16, 17, 19, 20, 21, 22	Not detected	4, 9
HBL_250	Not detected	Not detected	Not detected

CN gains at 14q11.2 (Fig. 3). Further, in RQ-PCR analysis, the CN gain of *EphB6* and *DAD1* was evident in all samples that showed high-grade amplification in SNP array (data not shown). Other high-grade amplifications are listed in Table 3. The size of these amplicons was typically less than 1 Mb, and the possible genes present in these regions are summarized in the same table. All these candidate genes, except *MMP7*, have not been reported previously with regard to HBL.[33]

Homozygous deletions are also of particular interest because they may indicate a tumor suppressor gene. However, homozygous deletions were not identified in any sample.

CN neutral LOH (UPD). LOH can be more sensitively detected with the CNAG/AsCNAR algorithms by evaluating the allele-specific CN than from the grossly reduced heterozygous SNP calls, particularly when the SNP shows no CN losses. The UPD regions were identified in five of the 17 samples. In four samples (HBL_7, HBL_28, HBL_37, and HBL_231), 11p15 was the common UPD region (Fig. 4a). Other UPD regions were observed within chromosomes 4, 9, and 16q22 (Table 2). The candidate target genes that map to the UPD region located within 11p15 include *IGF2* and *H19*. Methylation-specific PCR analysis was performed for the four HBL samples having UPD within 11p15 to identify the origin of the amplified allele. The methylation status of the differential methylated region (DMR) of *H19* is shown in Fig. 4b. Hypermethylation of the *H19* DMR was detected in all HBL samples having UPD within 11p15; however, normal lymphocyte DNA showed the mosaic methylation pattern. In general, the *H19* DMR is hypermethylated on the paternal allele

Table 3. High-grade amplifications in hepatoblastoma (HBL) samples

Cytoband	Implicated region (base pairs)		Candidate target genes in the region
	Start–end	Size	
2q34	211 193 864–212 239 181	1 045 318	*ErbB4*
3p25.2	11 888 124–12 876 175	988 052	*RAF1*
7q34	141 721 559–142 076 238	354 680	*EphB6*
11q22.2-q22.3	101 394 973–102 830 195	1 435 223	*MMP1, 7, 20*
14q11.2	21 426 631–22 130 392	703 762	*DAD1*

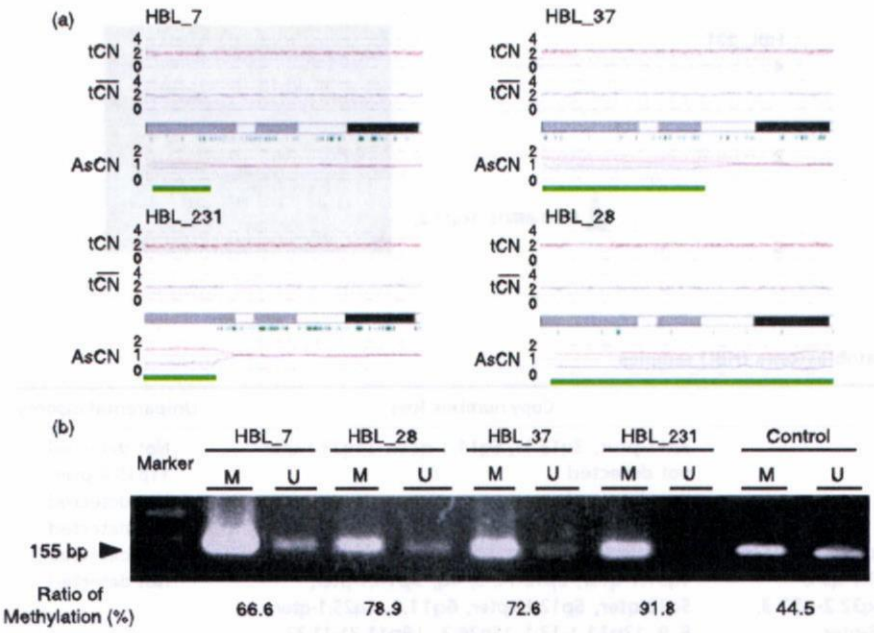

Fig. 4. (a) Copy numbers (CN) of chromosome 11p in four hepatoblastoma (HBL) samples with uniparental disomy (UPD). Although complete CN alterations are not observed, UPD is clearly predicted based on the allele-specific CN alterations (green lines). (b) Methylation-specific polymerase chain reaction (PCR) analysis of the *H19* differential methylated region (DMR). Modified DNA was amplified with primer pairs for methylated and unmethylated complete sequences of the *H19* DMR. *H19* DMR hypermethylation was detected in all HBL samples; however, normal lymphocyte DNA exhibited the mosaic methylation pattern. The results of quantitative real-time methylation-specific PCR analysis are shown below the image depicting the results of electrophoresis.

and hypomethylated on the maternally expressed allele in humans. This indicates that the UPD within this region is considered to be derived from the paternal allele. Furthermore, a low expression level of the non-methylated allele was also observed; methylation-specific RQ-PCR analysis revealed that the ratio of the methylation status ranged from 66.6% to 91.8%.

Expression analyses using RQ-RT-PCR. In order to examine the impact of the abovementioned amplifications and UPD on gene expression, we measured the expression levels of four genes (*DAD1*, *ErbB4*, *IGF2*, and *H19*) through RQ-RT-PCR (Fig. 5). Normal liver total RNA served as the non-neoplastic reference and control. HBL_184 and HBL_231 for which RNA were available showed a high expression of the *ErbB4* gene. However, the expression of *DAD1* was down-regulated in both these samples. The *IGF2* and *H19* genes were oppositely expressed between HBL_184 and HBL_231, having UPD within 11p15.

Discussion

The present study represents the application of the SNP array technology for the genome-wide analysis of CN aberrations in HBL. Several recent studies and our previous research have demonstrated that this technology provided a unique opportunity to assess the DNA CN alterations and LOH simultaneously throughout the entire genome.[24–27,29] As shown in the present analysis, the use of high-resolution SNP arrays improved the ability to identify structural chromosomal aberrations in cancer cells and detect genes affected by these aberrations. Additionally, high-density SNP array analysis with the CN analyzer software can also

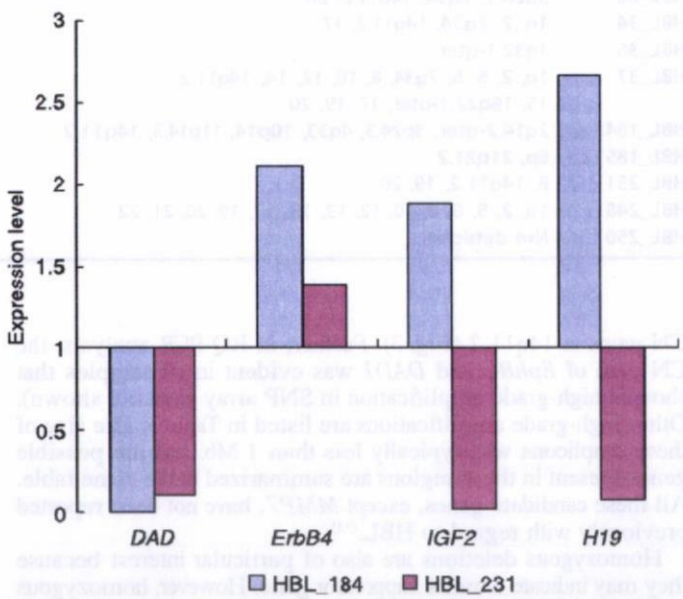

Fig. 5. The results of the expression levels of four genes (defender against cell death 1 [*DAD1*], EPH receptor B6 [*EphB6*], *ErbB4*, insulin-like growth factor II [*IGF2*], and *H19* genes) through real-time quantitative reverse transcription-polymerase chain reaction (RQ-RT-PCR) analyses.

doi: 10.1111/j.1349-7006.2007.00710.x